Cell Reports
Medicine

Article

Inhibition of polyamine biosynthesis preserves β cell function in type 1 diabetes

Graphical abstract

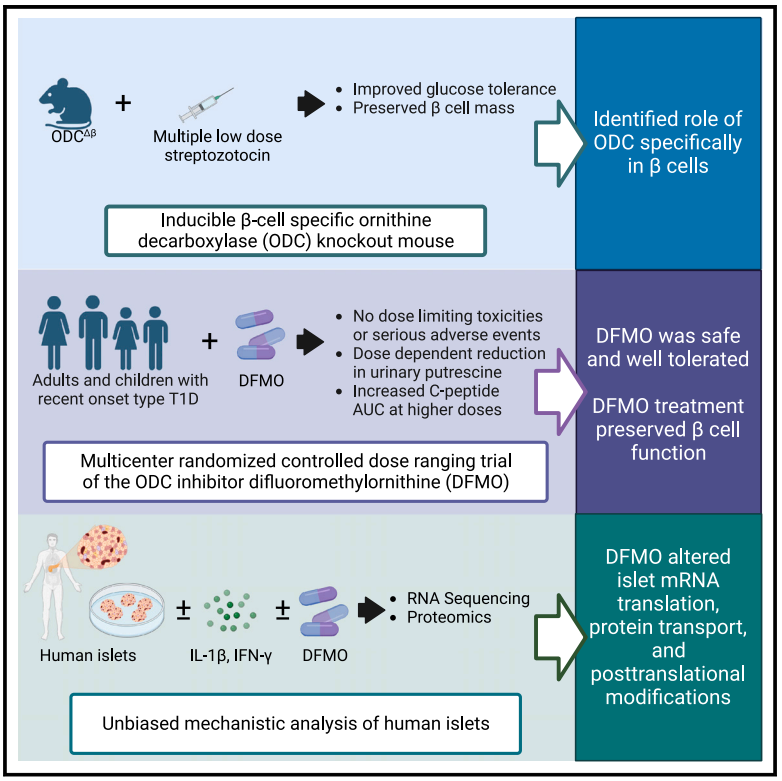

Highlights

- DFMO treatment is safe and preserves β cell function in subjects with T1D
- β cell knockout of the DFMO target ODC in mice reduces hyperglycemia
- DFMO treatment of human islets influences protein production and release pathways

Authors

Emily K. Sims, Abhishek Kulkarni, Audrey Hull, ..., Eugene W. Gerner, Raghavendra G. Mirmira, Linda A. DiMeglio

Correspondence

eksims@iu.edu (E.K.S.), mirmira@uchicago.edu (R.G.M.)

In brief

Sims et al. integrate experiments with β cell-specific knockout mice and human islets *in vitro* alongside a multicenter clinical trial to show that inhibition of polyamine biosynthesis is a safe approach to protect β cell function in individuals with recent-onset type 1 diabetes.

Sims et al., 2023, Cell Reports Medicine *4*, 101261
November 21, 2023
https://doi.org/10.1016/j.xcrm.2023.101261

CellPress

Cell Reports Medicine

CellPress
OPEN ACCESS

Article

Inhibition of polyamine biosynthesis preserves β cell function in type 1 diabetes

Emily K. Sims,[1,*] Abhishek Kulkarni,[2] Audrey Hull,[1,3] Stephanie E. Woerner,[1] Susanne Cabrera,[4] Lucy D. Mastrandrea,[5] Batoul Hammoud,[6] Soumyadeep Sarkar,[7] Ernesto S. Nakayasu,[7] Teresa L. Mastracci,[8] Susan M. Perkins,[9] Fangqian Ouyang,[9] Bobbie-Jo Webb-Robertson,[7] Jacob R. Enriquez,[2] Sarah A. Tersey,[2] Carmella Evans-Molina,[1,10,11] S. Alice Long,[12] Lori Blanchfield,[12] Eugene W. Gerner,[13] Raghavendra G. Mirmira,[2,6,14,*] and Linda A. DiMeglio[1]

[1]Division of Pediatric Endocrinology and Diabetology, Herman B. Wells Center for Pediatric Research, Center for Diabetes and Metabolic Diseases, Indiana University School of Medicine, Indianapolis, IN 46202, USA
[2]Kovler Diabetes Center and Department of Medicine, The University of Chicago, Chicago, IL 60637, USA
[3]Nationwide Children's Hospital Pediatric Residency Program, Columbus, OH 43205, USA
[4]Department of Pediatrics, Section of Endocrinology and Diabetes, Medical College of Wisconsin, Milwaukee, WI 53226, USA
[5]Division of Pediatric Endocrinology, Jacobs School of Medicine and Biomedical Sciences, University at Buffalo, Buffalo, NY 14203, USA
[6]Department of Pediatrics, The University of Chicago, Chicago, IL 60637, USA
[7]Biological Sciences Division, Pacific Northwest National Laboratory, Richland, WA 99354, USA
[8]Department of Biology, Indiana University-Purdue University Indianapolis, Indianapolis, IN 46202, USA
[9]Department of Biostatistics and Health Data Science, Indiana University School of Medicine, Indianapolis, IN 46202, USA
[10]Department of Medicine and the Herman B. Wells Center for Pediatric Research, Indiana University School of Medicine, Indianapolis, IN 46202, USA
[11]Roudebush VA Medical Center, Indianapolis, IN 46202, USA
[12]Benaroya Research Institute, Center for Translational Immunology, Seattle, WA 98101, USA
[13]Cancer Prevention Pharmaceuticals, Tucson, AZ 85718, USA
[14]Lead contact
*Correspondence: eksims@iu.edu (E.K.S.), mirmira@uchicago.edu (R.G.M.)
https://doi.org/10.1016/j.xcrm.2023.101261

SUMMARY

In preclinical models, α-difluoromethylornithine (DFMO), an ornithine decarboxylase (ODC) inhibitor, delays the onset of type 1 diabetes (T1D) by reducing β cell stress. However, the mechanism of DFMO action and its human tolerability remain unclear. In this study, we show that mice with β cell ODC deletion are protected against toxin-induced diabetes, suggesting a cell-autonomous role of ODC during β cell stress. In a randomized controlled trial (ClinicalTrials.gov: NCT02384889) involving 41 recent-onset T1D subjects (3:1 drug:placebo) over a 3-month treatment period with a 3-month follow-up, DFMO (125–1,000 mg/m^2) is shown to meet its primary outcome of safety and tolerability. DFMO dose-dependently reduces urinary putrescine levels and, at higher doses, preserves C-peptide area under the curve without apparent immunomodulation. Transcriptomics and proteomics of DFMO-treated human islets exposed to cytokine stress reveal alterations in mRNA translation, nascent protein transport, and protein secretion. These findings suggest that DFMO may preserve β cell function in T1D through islet cell-autonomous effects.

INTRODUCTION

Type 1 diabetes (T1D) is an autoimmune disorder that destroys insulin-producing pancreatic β cells.[1] Although therapy has greatly improved over the past century,[2] morbidity and mortality as well as costs and impacts on quality of life remain burdensome for affected individuals.[3–6] There is a clear need for safe, effective disease-modifying therapies that address underlying pathologic etiologies. Such therapies might not only improve residual endogenous insulin secretion, which is associated with improved disease outcomes,[7] but also, when given early enough in the disease process, have the potential to delay T1D onset and the need for exogenous insulin.[8]

A growing body of work suggests that activation of stress-responsive pathways within the β cell contributes to or exacerbates autoimmune-associated β cell dysfunction and death in T1D.[9] One such pathway is the tightly regulated polycationic aliphatic amine (polyamine) biosynthesis pathway, implicated in a variety of cellular functions, including inflammatory responses and autoimmune disease, including T1D (Figure 1A).[10] Polyamines generated in β cells promote cytokine-induced inflammatory responses, in part through posttranslational activation of the proinflammatory translational factor eukaryotic translation initiation factor 5A (eIF5A).[11–13] In addition, high polyamine concentrations are present in B and T cells, suggesting that polyamines themselves and/or eIF5A contribute to progression of autoimmune diseases.[14–17] Notably, in the non-obese diabetic

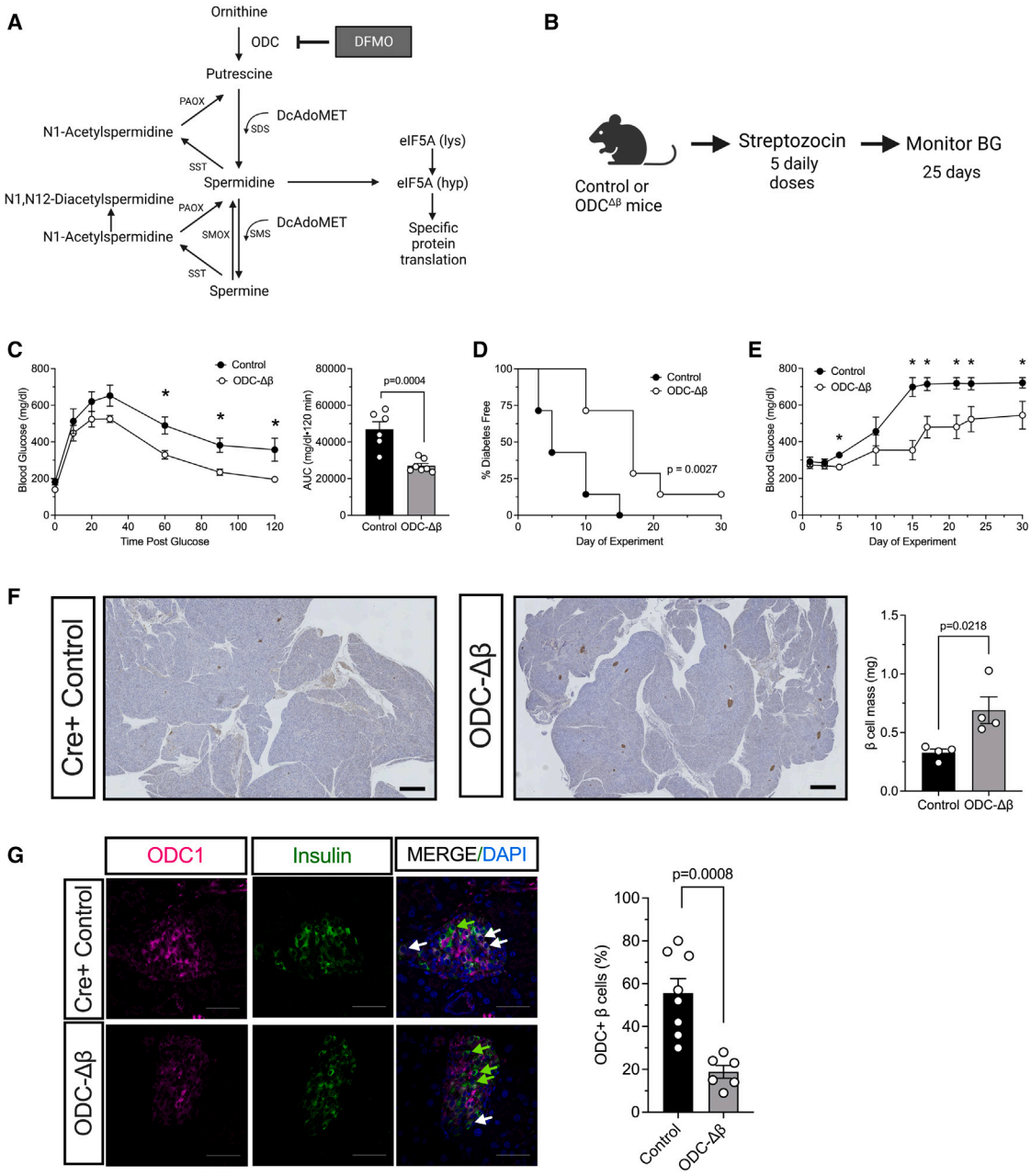

Figure 1. The polyamine biosynthetic pathway and the glycemic response of *Odc1*$^{\Delta\beta}$ mice to multiple low doses of STZ

(A) The polyamine metabolic pathway in mammals. Polyamine production is governed by the biosynthetic enzymes ornithine decarboxylase (ODC), spermidine synthase (SPS), and spermine synthase (SMS) and the catabolic enzymes spermidine/spermine N1-acetyltransferase (SSAT), the flavin-dependent polyamine oxidase (PAOX), and spermine oxidase (SMOX). Spermidine is used as a substrate in the enzymatic modification of Lys50 in the protein eIF5A to generate the hypusine modification. Difluoromethylornithine (DFMO) is an irreversible inhibitor of ODC.

(B) A schematic showing the multiple low-dose streptozotocin (STZ) experiments. Male *Odc1*$^{\Delta\beta}$ mice and control Cre+ littermates were injected with STZ daily for 5 days. Subsequently, glucose levels and glucose tolerance were monitored.

(C) Glucose tolerance test and corresponding AUC analysis on day 10 after the start of STZ injections.

(D) Diabetes incidence; mice were considered to have diabetes after two consecutive blood glucose values of 250 mg/dL.

(E) Non-fasting blood glucose values over time.

(F) Representative immunohistochemistry images of pancreata showing β cells (insulin, brown) and hematoxylin (nuclei, blue) and corresponding β cell mass; scale bar, 200 μm.

(G) Representative immunofluorescence images of islets showing ODC (magenta), insulin (green), and nuclei (DAPI, blue) and corresponding percentage of β cells positive for ODC; scale bar, 50 μm.

n = 6–8 biological replicates. Data are presented as mean ± SEM. *p < 0.05 as indicated.

(NOD) mouse, a model of autoimmune T1D, administration of α-difluoromethylornithine (DFMO, an irreversible inhibitor of the polyamine biosynthetic enzyme ornithine decarboxylase [ODC]) delayed diabetes onset,[11] whereas administration of the polyamine spermidine increased the incidence of diabetes.[18] Moreover, in zebrafish, DFMO enhances β cell regeneration,[19] suggesting that depletion of polyamines might contribute to new β cell growth in some species.

Polyamines and their downstream modification of eIF5A also promote the production of proteins involved in cellular proliferation and growth.[20] For this reason, intravenous DFMO (also known clinically as eflornithine) has been approved by the US Food and Drug Administration (FDA) for treatment of trypanosomiasis,[21] and topical DFMO has been approved for an indication of hair removal,[22] with orphan drug designations for oral DFMO in multiple cancer types, including neuroblastoma, colon, gastric, and pancreatic cancers.[23–25] Although no oral indications are currently FDA approved, oral dosing has been investigated in recent clinical trials to prevent cancer relapse or treat cancers in adults and children, with a relatively favorable safety profile.[26–29] Based on preclinical data suggesting a role of polyamines in autoimmunity and cytokine-induced inflammation and an effect of DFMO *in vivo* to delay diabetes in NOD mice, we sought to clarify a direct role of ODC as a mechanism of disease in β cell stress and, as a clinical proof of principle, to examine whether oral DFMO treatment would safely improve β cell health in human T1D. We studied mice containing a β cell-specific knockout of the gene encoding ODC (*Odc1*), and examined safety, tolerability, and β cell outcomes of a dose-ranging, randomized controlled study of oral DFMO administration in pediatric and adult participants with recent-onset T1D. To identify mechanisms of action on human β cells, we also analyzed the transcriptomic and proteomic responses of stressed human islets treated with DFMO. Our findings suggest that ODC in β cells contributes to cell stress and that its inhibition in human islets promotes cell survival. In our initial human study, DFMO administration is safe and well tolerated at all doses tested, with evidence of efficacy to preserve C-peptide secretion at the highest tested doses.

RESULTS

Generation and analysis of β cell-specific Odc1-deficient mice

To study the role of *Odc1* in the postnatal β cells, we generated mice in which exons 2–12 of the *Odc1* allele were flanked by Cre recombinase recognition sequences (*loxP*) (Figure S1A). These mice were backcrossed for 10 generations onto the *C57BL6/J* background and then crossed to *C57BL6/J* mice harboring a transgene encoding the Cre recombinase-modified estrogen receptor fusion protein under control of the mouse *Ins1* promoter (*MIP1-CreERT*).[30] Mouse genotypes were confirmed by polymerase chain reaction (PCR) genotyping (Figures S1B and S1C). Administration of tamoxifen to $Odc1^{loxP/loxP}$;*MIP1-CreERT* mice at 8 weeks of age resulted in the generation of β cell-specific *Odc1* knockout mice ($Odc1^{\Delta\beta}$). One week following tamoxifen injections, no alterations in glucose tolerance (by intraperitoneal glucose tolerance test) were observed in $Odc1^{\Delta\beta}$ mice compared with littermate controls (Figure S1D), a finding suggesting that the acute loss of ODC in adult β cells does not affect glucose homeostasis at this age and under these experimental conditions.

To interrogate the role of ODC in β cell stress, we next subjected $Odc1^{\Delta\beta}$ mice and littermate controls (a combination of *MIP1-CreERT*+ and $Odc1^{loxP/loxP}$ controls) to multiple low-dose streptozotocin (STZ) injections (see scheme in Figure 1B). The multiple low-dose STZ injections (55 mg/kg body weight STZ × 5 days) mimic the inflammatory milieu of T1D, in which animals develop local islet inflammation and resultant hyperglycemia over time.[31,32] 10 days following the start of STZ injections, $Odc1^{\Delta\beta}$ mice exhibited improved glucose tolerance compared with controls (Figure 1C), and glucose tolerance remained improved 20 days following the start of STZ injection (Figure S1E). As glucose levels were followed over the course of 25 days post STZ injections, $Odc1^{\Delta\beta}$ mice exhibited delayed development of diabetes (as defined by glucose levels >250 mg/dL) (Figure 1D) and significantly lower blood glucose levels (Figure 1E) compared with control littermates. We measured proinsulin:insulin ratios (with higher ratios reflecting more β cell stress)[33] at the end of the study but did not observe any significant difference between control and $Odc1^{\Delta\beta}$ animals (Figure S1F). β Cell mass at the end of the study was significantly (2-fold) higher in $Odc1^{\Delta\beta}$ mice compared with controls (Figure 1F). Collectively, these data are consistent with those reported previously for animals that received the oral ODC inhibitor DFMO.[11] To verify the deletion of *Odc1* in $Odc1^{\Delta\beta}$ mice, we performed immunostaining for ODC in islets. As shown in Figure 1G, there was an ∼65% reduction in the number of β cells exhibiting ODC production in $Odc1^{\Delta\beta}$ mice compared with controls. This reduction is consistent with our previously reported recombination efficiency of the *MIP1-CreERT* transgene.[34] Collectively, the data in Figures 1 and S1 indicate that ODC contributes to a pathway in β cells that impedes their function and survival in the setting of cellular stress.

Clinical trial of DFMO in persons with T1D

The aforementioned findings of β cell ODC deletion in mice and the previous studies of ODC inhibition with DFMO in NOD mice led us to assess the safety and potential β cell preservation effects of DFMO in persons with T1D. We enrolled 41 participants in an interventional study between May 4, 2015 and June 25, 2019, with 31 individuals treated at one of 5 doses of DFMO orally and 10 treated with placebo (see the schematic in Figure 2A, the CONSORT diagram in Figure S2, and the schedule of events in Table S1). The last visit for the final participant was on October 7, 2019. The primary endpoint was safety, with prespecified secondary analyses including measurement of mixed-meal stimulated β cell function (C-peptide area under the curve [AUC]) and β cell stress (proinsulin:C-peptide ratio), and urinary polyamines. Baseline characteristics of study participants, including demographics, autoantibody positivity, duration of diabetes, and metabolic measurements at the time of randomization, are shown in Table 1. Of 41 total participants, 31 (83%) were children under 18 years of age. Two participants withdrew from the study. The first participant (in the 750 mg/m^2 active drug group) withdrew because of development of a diffuse urticarial rash and symptoms of anaphylaxis that developed slightly over 2 weeks after drug

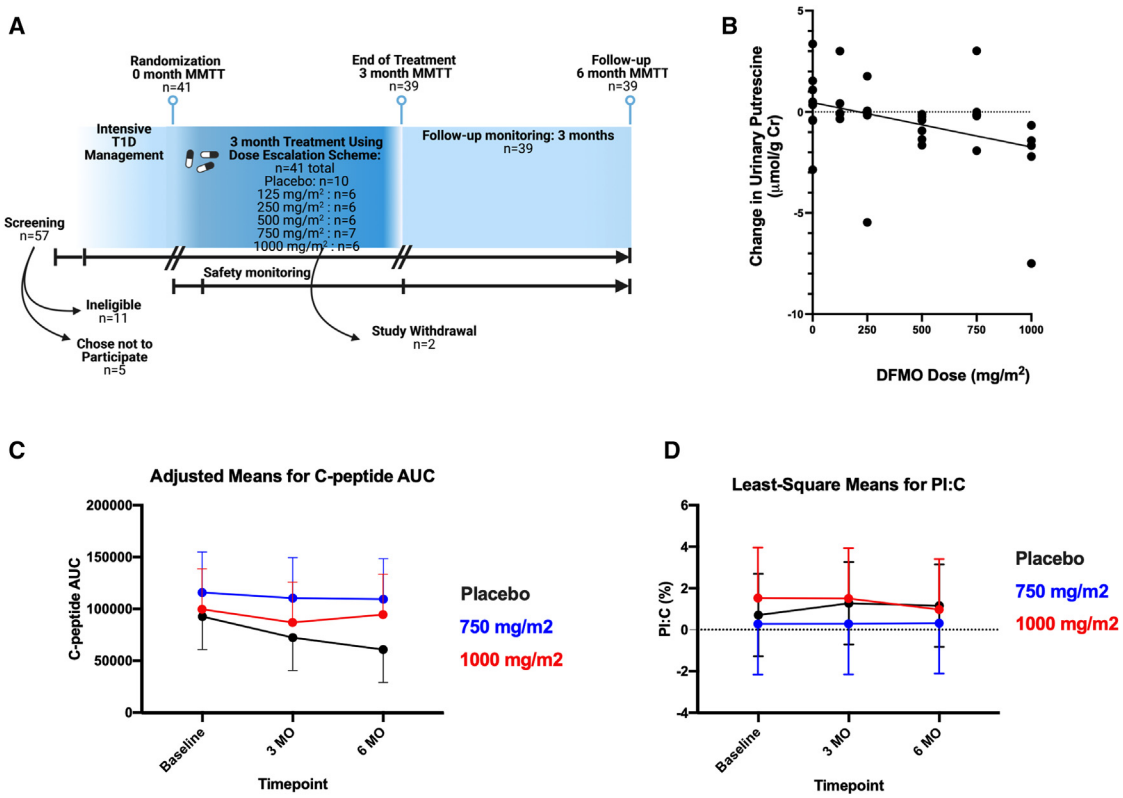

Figure 2. Key features of study design and findings

(A) CONSORT diagram for participants in this trial.

(B) Scatterplot showing significant correlation (Pearson r = −0.385; p = 0.02) between DFMO dose (x axis) vs. change in urinary putrescine, the direct downstream product of ODC (y axis).

(C and D) Least square means, modeled with ANCOVA using baseline values as a covariate, for (C) mixed-meal C-peptide AUC and (D) fasting proinsulin:C-peptide ratios (PI:C) for participants in the placebo and 1,000 mg/m^2/day dosing groups at baseline, after 3 months of treatment, and at the 6-month follow-up visit.

Data are presented as least square means ± 95% confidence interval. Sample size for each group was as follows: placebo, n = 10; 125 mg/m^2, n = 6; 250 mg/m^2, n = 6; 500 mg/m^2, n = 6; 750 mg/m^2, n = 7; 1,000 mg/m^2, n = 6.

administration. The second participant was randomized to the placebo group and withdrew during the 3-month end-of-treatment mixed meal tolerance test (MMTT) because of issues obtaining intravenous access for MMTT blood collection.

Safety of DFMO in persons with T1D

No *a priori* defined dose-limiting toxicities or serious (>grade 2) adverse events (AEs) were observed in any study participants at any of the drug doses. No participants exhibited hearing loss on audiogram testing (>25-dB increase in threshold). All AEs reported are shown in Table 2, and AEs judged by masked investigators as having a possible or probable relationship to the study drug are shown in Table S2. Grouped AEs occurring on the same day (for example, congestion, cough, and report of an upper respiratory infection (URI)) were counted individually and as part of an AE episode. A total of 57 AE episodes were reported by participants in the active drug group (31 total participants; 1.8 AEs/participant) compared with 12 total episodes in the placebo group (10 total participants, 1.2 AEs/participant). AEs occurred more commonly with higher doses of drug; for the 750 mg/m^2 group, 2.8 episodes/participant were reported, and for the 1,000 mg/m^2 group, 2.7 episodes/participant were reported. These most commonly included mild gastrointestinal symptoms, mild anemia, mild-moderate headache, and mild-moderate symptoms associated with a viral infection or URI. As noted above, one participant had an urticarial reaction to the drug. Eight other moderate AE episodes were reported in participants on the drug, including a head injury while skiing; a migraine with associated dizziness and anxiety; an isolated headache; a pump site infection; nasal congestion; an upper respiratory illness; an upper respiratory illness with associated congestion, cough, sore throat, and headache; a viral illness with headache, nausea, and hot flashes; and a rash related to poison ivy. No unexpected AEs judged to be possibly related to drug therapy occurred.

Eleven individuals reported gastrointestinal symptom episodes during the study. These included 2 participants in the placebo group, 1 participant in the 100 mg/m^2 dosing group, 2 participants in the 250 mg/m^2 dosing group, 3 participants in the 750 mg/m^2 dosing group, and 3 participants in the 1,000 mg/m^2 dosing group. These were all rated as mild and

Table 1. Baseline study participant characteristics

Variable	Placebo (n = 10)	125 mg/m^2 (n = 6)	250 mg/m^2 (n = 6)	500 mg/m^2 (n = 6)	750 mg/m^2 (n = 7)	1,000 mg/m^2 (n = 6)
Age (years)	16.5 (6.5)	17.0 (6.3)	15.0 (2.7)	15.5 (2.6)	16.2 (5.3)	15.7 (2.3)
Race (%)						
Black	0 (0.0%)	0 (0.0%)	0 (0.0%)	0 (0.0%)	1 (14.3%)	0 (0.0%)
Multiple	1 (10.0%)	0 (0.0%)	0 (0.0%)	0 (0.0%)	1 (14.3%)	0 (0.0%)
White	9 (90.0%)	6 (100%)	6 (100%)	6 (100%)	5 (71.4%)	6 (100%)
Number female (%)	5 (50.0%)	1 (16.7%)	3 (50.0%)	1 (16.7%)	4 (57.1%)	3 (50.0%)
BMI (kg/m2)	22.8 (2.9)	21.4 (2.8)	22.1 (4.6)	27.0 (7.2)	23.9 (4.4)	21.1 (3.2)
HbA1c % [mmol/mol]	7.9 (1.4) [63]	7.4 (1.5) [57]	6.7 (1.3) [50]	6.0 (0.3)* [42]	6.2 (0.7)* [44]	7.2 (1.8) [55]
Days since T1D diagnosis	156.3 (63.5)	166.7 (71.4)	125.7 (58.0)	148.0 (68.4)	128.6 (50.0)	86.8 (29.4)*
Insulin regimen (%)						
1–2 injections/day	1 (10.0%)	0 (0.0%)	0 (0.0%)	1 (16.7%)	1 (14.3%)	1 (16.7%)
3+ injections daily	8 (80.0%)	5 (83.3%)	4 (66.7%)	5 (83.3%)	4 (57.1%)	4 (66.7%)
Pump	1 (10.0%)	1 (16.7%)	2 (33.3%)	0 (0.0%)	2 (28.6%)	1 (16.7%)
Number using CGMs (%)	2 (20.0%)	1 (16.7%)	1 (16.7%)	2 (33.3%)	3 (42.9%)	2 (33.3%)
C-peptide AUC (pmol/L)	90,357.2 (45,452.3)	78,396.0 (49,915.9)	90,189.2 (34,964.4)	116,417 (28,123.8)	125,869 (70,919.1)	99,902.7 (35,720.9)
Glucose AUC (mg/dL)	34,045.5 (8,800.2)	28,032.8 (10,928.9)	27,076.7 (8,006.3)	23,844.6* (2,033.7)	23,217.6* (4,205.7)	26,990.1 (6,748.8)
Fasting PI:C (%)	0.8 (0.7)	0.8 (0.6)	1.2 (0.8)	1.0 (1.1)	0.3 (0.2)	1.5 (1.0)
GADA positive (%)	8 (80.0%)	6 (100%)	4 (66.7%)	6 (100%)	7 (100%)	5 (83.3%)
IA-2 positive (%)	5 (50.0%)	5 (83.3%)	6 (100%)	4 (66.7%)	6 (85.7%)	3 (50.0%)
IAA positive (%)	7 (70.0%)	4 (66.7%)	5 (83.3%)	5 (83.3%)	7 (100%)	5 (83.3%)
ZnT8A positive (%)	5 (50.0%)	2 (33.3%)	6 (100%)	4 (66.7%)	4 (57.1%)	2 (33.3%)
N1,12-diacetylspermine (μmol/g Cr)	0.3 (0.3)	0.2 (0.1)	0.3 (0.2)	0.2 (0.1)	0.3 (0.1)	0.1 (0.1)
N1-acetylspermidine (μmol/g Cr)	4.7 (2.9)	3.6 (1.0)	4.6 (2.4)	3.5 (1.6)	4.3 (2.9)	3.9 (2.2)
N8-acetylspermidine (μmol/g Cr)	3.5 (1.2)	3.6 (1.1)	4.2 (1.5)	3.7 (1.6)	3.7 (0.7)	3.8 (1.1)
Putrescine (μmol/g Cr)	1.2 (1.1)	1.1 (1.2)	1.6 (2.4)	1.1 (0.8)	0.9 (0.7)	3.1 (3.0)
DcAdoMet (μmol/g Cr)	0.2 (0.0)	0.2 (0.1)	0.2 (0.1)	0.2 (0.1)	0.2 (0.1)	0.2 (0.1)

Data are shown as mean (standard deviation) for continuous variables or absolute number (%) for categorical variables. BMI, body mass index; CGM, continous glucose monitoring; GADA, glutamic acid decarboxylase 65 antibody; IA-2, islet antigen 2 autoantibody; IAA, insulin autoantibody; ZnT8A, zinc transporter 8 autoantibody; Cr, creatinine. *$p < 0.05$ compared with values for the placebo group.

were typically self-limited. No episodes led to discontinuation of the drug.

Because hematopoietic suppression was considered a potential dose-limiting toxicity of concern, we further examined cases of anemia among study participants (Table S3). Episodes of mild anemia occurred in 7 participants over the course of the study: 2 in the placebo group, 2 in the 250 mg/m^2 dosing group, 1 in the 750 mg/m^2 dosing group, and 2 in the 1,000 mg/m^2 dosing group. Among participants on active drug, 4 of 5 exhibited the lowest hemoglobin values at the randomization visit, with improved or stable values at the next blood draw, suggesting that anemia was not causally related to DFMO dosing. One participant, in the 750 mg/m^2 dosing group, exhibited a hemoglobin value in the normal range throughout the study but did have a hematocrit value below the reference range at the first safety assessment on treatment. This value normalized by the end of the 3-month treatment period.

Target engagement of DFMO in persons with T1D

To verify that DFMO administration inhibited ODC as expected, the effect of each dosing regimen on urinary polyamines was assessed. Levels at the 3-month time point were modeled using analysis of covariance (ANCOVA) with adjustment for baseline values (all values are provided in Table 3). Here, compared with placebo, we observed absolute decreases in average urinary putrescine, the direct product of ODC (Figure 1A), with DFMO treatment for all treatment groups, with significant or near-significant differences in the 500 ($p = 0.03$) and 1,000 mg/m^2 ($p = 0.05$) dosing groups. Overall, higher doses of DFMO correlated with larger reductions in urinary putrescine (Pearson $r = -0.385$, $p = 0.02$) (Figure 2B). With higher doses in the 750 mg/m^2 and 1,000 mg/m^2 groups, we also observed trends ($p = 0.09$) toward increased values of decarboxylated S-adenosylmethionine (DcAdoMet), a necessary substrate of spermidine that would be expected to increase in the context of reduced putrescine. No significant differences

Table 2. All adverse events (AEs)

AE	Placebo (n = 10)	Cohort 1, 125 mg/m^2 (n = 6)	Cohort 2, 250 mg/m^2 (n = 6)	Cohort 3, 500 mg/m^2 (n = 6)	Cohort 4, 750 mg/m^2 (n = 7)	Cohort 5, 1,000 mg/m^2 (n = 6)
Gastrointestinal	2	2	3	0	5	3
Nausea	2	0	0	0	3	0
Vomiting	1	2	0	0	0	1
Diarrhea	0	0	2	0	0	1
Abdominal pain	1	1	2	0	2	1
Nausea with IV placement	0	0	0	0	1	0
Constipation	0	0	0	0	1	0
Decreased appetite	0	0	1	0	0	0
Hematologic						
ANC In CTCAE 1	2	1	0	0	0	0
Anemia	2	0	2	0	1	2
Neurologic	0	1	0	0	2	2
Headache	0	1	0	0	1	2
Dizziness	0	0	0	0	2	0
Viral illness	3	0	6	0	5	6
Congestion	3	0	0	0	2	2
Cough	3	0	0	0	0	1
Headache	2	0	1	0	1	2
Sore throat	0	0	0	0	0	1
Fever	0	0	3	0	0	1
Dizziness	0	0	0	0	3	0
Fatigue	0	0	1	0	0	0
Hot flashes associated with viral illness	0	0	0	0	0	1
Upper respiratory illness	2	0	3	0	2	3
Other viral illness	0	0	0	0	1	2
Other infectious/immune						
Pump site infection	0	0	0	0	1	1
Paronychia of digit	0	0	0	0	3	0
Enlarged lymph node	0	0	0	0	0	1
Other						
Hypoglycemia	1	0	0	1	0	0
Hyperglycemia	0	0	1	0	0	0
Increased thirst	0	0	0	1	0	0
Polyuria	0	0	0	1	0	0
Urticaria with systemic reaction	0	0	0	0	1	0
Wisdom tooth extraction	1	0	0	0	0	0
Cut finger	1	0	0	0	0	0
Anxiety	0	0	0	0	1	0
Ankle fracture	0	0	1	0	1	0
Poison ivy	0	0	0	0	0	1
Shoulder injury	0	0	1	0	0	0
Head injury skiing	0	0	1	0	0	0
Syncope after taking marijuana	0	1	0	0	0	0
Loss of appetite attributed to personal problems	0	0	1	0	0	0

(*Continued on next page*)

Table 2. *Continued*

AE	Placebo (n = 10)	Cohort 1, 125 mg/m^2 (n = 6)	Cohort 2, 250 mg/m^2 (n = 6)	Cohort 3, 500 mg/m^2 (n = 6)	Cohort 4, 750 mg/m^2 (n = 7)	Cohort 5, 1,000 mg/m^2 (n = 6)
Total episodes	12	5	14	2	20	16
Total episodes/participant	1.2	0.8	2.3	0.3	2.9	2.7
Number of participants reporting AEs	7	3	4	1	7	5

ANC, absolute neutrophil count;
CTCAE, common terminology criteria for AEs.

with DFMO treatment were observed in urinary levels of N1- or N8-acetylspermidine, or N1,12-diacetylspermine.

Efficacy of DFMO in persons with T1D

To assess the treatment efficacy of DFMO, we evaluated hemoglobin A1c (HbA1c) values as a glycemic measure at the completion of treatment (Table S4) as well as glucose AUC on MMTT and measures of β cell function (C-peptide AUC on MMTT) at the randomization, 3-month, and 6-month study time points (Table 4). At the end of treatment (3 months), no significant differences in HbA1c values were noted in any of the treatment groups relative to placebo. MMTT-derived adjusted means for C-peptide AUC and glucose AUC values are shown for each dosing group at both time points in Table 4. Here, no significant differences between placebo-treated and DFMO-treated participants were observed at the 3-month time point. However, by the 6-month time point after randomization, compared with placebo, MMTT C-peptide AUC values were significantly higher in the 125 mg/m^2 ($p = 0.02$), 750 mg/m^2 ($p = 0.03$), and 1,000 mg/m^2 DFMO dosing groups ($p = 0.02$; longitudinal data in Figure 2C). MMTT glucose AUC values were not significantly different between any of the groups at the 3-month time point and were only significantly lower in the 125 mg/m^2 ($p = 0.03$) and 750 mg/m^2 ($p = 0.02$) treatment groups compared with placebo at the 6-month time point.

We also obtained fasting proinsulin-to-C-peptide ratios (PI:C), a biomarker of β cell stress,[35,36] at the randomization, 3-month, and 6-month study time points (Table 4). Similar to C-peptide AUC and glucose AUC, no significant differences in fasting PI:C were noted between placebo-treated and DFMO-treated groups at the 3-month time point. 6 months after randomization, although absolute PI:C values progressively decreased with increasing DFMO dosing, only the 1,000 mg/m^2 group exhibited a decrease in the PI:C compared with placebo ($p = 0.04$; longitudinal data in Figure 2D).

Given the potential role of polyamines in immune cell activation, we also performed peripheral blood mononuclear cell (PBMC) immunophenotyping before and after treatment. No significant treatment-mediated changes in immune cell subsets or phenotypes, including Treg, Th17, or other CD4$^+$ or CD8$^+$ T cells were noted. Changes were equivalent between percent coefficient of variation (CV) at baseline and on treatment (Figure S3).

Inhibition of ODC in human islets alters the molecular response to inflammation

To interrogate the molecular effects by which ODC inhibition might result in human β cell protection, we next performed unbiased RNA sequencing analysis of human islets from 5 donors (see donor characteristics in Table S5). Human islets were either treated with vehicle or the ODC inhibitor DFMO or treated with vehicle or DFMO in the presence of proinflammatory cytokines (interleukin-1β [IL-1β] + interferon γ [IFN-γ]) (to ascertain the effect of DFMO under conditions of T1D inflammation) (Figure 3A). Hierarchical clustering analysis of the RNA sequencing outputs (see Table S6 for the complete RNA sequencing dataset) indicated that replicates clustered largely by cytokine treatment with little effect of DFMO (Figure 3B). When using a fold change (FC) greater than 2 and false discovery rate (FDR) less than 0.05, only 15 genes (of 25,382 identified) reached the differential expression threshold (volcano plot, Figure 3C) upon DFMO treatment of human islets, and none of these genes clustered in functional Gene Ontology (GO) pathway terms that reached statistical significance. Similarly, only 55 genes reached the differential expression threshold upon DFMO treatment of cytokine-exposed human islets (volcano plot, Figure 3D), also with no significant clustering by GO pathway terms. By contrast, when the significance threshold was lowered to $p < 0.05$ (with $FC > 2$), 622 genes were altered by DFMO treatment alone, and 785 genes were altered by DFMO in the presence of cytokines. GO terms that correlated with the effect of DFMO in the presence of cytokines included processes related to protein and nucleic acid metabolism, posttranscriptional gene regulation, and mRNA translation (Figure S1E)—processes in which polyamines are known to participate.[37]

Given the minimal changes observed in transcriptomics and the suggestion that these changes might relate to mRNA translation, we next performed unbiased data-independent acquisition mass spectrometry-based proteomics of human islets. Human islets from 6 donors were treated in groups identical to those used for RNA sequencing (Table S5). Principal-component analysis demonstrated that samples largely clustered by donor, with the effect of cytokines on both dimensions of principal components and the effect of DFMO primarily on the vertical dimension (principal component 2) of the plot (Figure 3E). A total of 616 proteins (of 8751 identified) were significantly altered ($FDR < 0.05$) in the presence of DFMO, and 701 proteins were altered in the presence of cytokines and DFMO (Figures 3F and 3G, volcano plots) (see Table S6 for the complete proteomics dataset). GO terms linked to the altered proteins under non-cytokine conditions included regulation of cellular apoptosis and proliferation, posttranscriptional regulation of gene expression, protein maturation and modification, and regulation of hormone levels

Table 3. Urinary polyamines

Measure	3-month time point		
	Drug dose (mg/m^2)	Least square means (95% CI)	p Value
N1-acetylspermidine (μmol/g Cr)	0	3.37 (2.53, 4.20)	–
	125	3.43 (2.38, 4.48)	0.93
	250	3.30 (2.34, 4.25)	0.91
	500	2.87 (1.91, 3.82)	0.43
	750	1.94 (0.99, 2.89)	0.03
	1,000	2.89 (1.85, 3.93)	0.47
N8-acetylspermidine (μmol/g Cr)	0	3.46 (3.01, 3.90)	–
	125	3.60 (3.03, 4.16)	0.69
	250	3.58 (3.06, 4.10)	0.72
	500	3.27 (2.76, 3.79)	0.59
	750	2.84 (2.33, 3.35)	0.07
	1,000	2.88 (2.32, 3.45)	0.11
N1,12-diacetylspermine (μmol/g Cr)	0	0.17 (0.12, 0.22)	–
	125	0.16 (0.10, 0.23)	0.91
	250	0.21 (0.15, 0.27)	0.33
	500	0.18 (0.12, 0.24)	0.78
	750	0.23 (0.17, 0.29)	0.13
	1,000	0.21 (0.14, 0.28)	0.33
Putrescine (μmol/g Cr)	0	1.64 (0.87, 2.42)	–
	125	1.19 (0.19, 2.19)	0.47
	250	0.88 (−0.02, 1.78)	0.20
	500	0.29 (−0.61, 1.19)	0.03
	750	1.01 (0.10, 1.91)	0.28
	1,000	0.31 (−0.75, 1.38)	0.05
DcAdoMet (μmol/g Cr)	0	0.22 (0.15, 0.30)	–
	125	0.25 (0.16, 0.34)	0.60
	250	0.23 (0.15, 0.31)	0.92
	500	0.22 (0.14, 0.31)	0.99
	750	0.32 (0.24, 0.40)	0.09
	1,000	0.33 (0.23, 0.42)	0.09

Least square means adjusted for baseline value.

(Figure 3H). GO terms under conditions of proinflammatory cytokine treatment (Figure 3I) similarly reflected molecular events related to mRNA processing and translation initiation, endoplasmic reticulum and Golgi transport, protein modification, vesicle transport, and exocytosis. Collectively, these findings implicate mRNA translation, protein transport, and posttranslational modifications as effects induced by DFMO treatment (Figure 3J). These posttranscriptional events have been implicated as processes promoting β cell dysfunction and immunogenicity in T1D.[38]

DISCUSSION

Polyamines are ubiquitous bioactive amines that participate in numerous cellular functions, including cellular differentiation, replication, and mRNA translation.[10,20] It has long been known that polyamine concentrations are elevated in the pancreas, particularly in β cells, where they may support the production of proteins in highly secretory cell types,[39,40] but their participation in diabetes pathogenesis has not been fully explored. The enzyme ODC is one of the key enzymes that participate in the production of polyamines and is the enzyme that directly regulates the production of the polyamine putrescine (Figure 1A). Genetic deletion of *Odc1* in mice is embryonically lethal,[41] thereby precluding study of its role in developing tissues. Conditional deletion of *Odc1* in macrophages of mice demonstrated its role in the regulation of M1-like, proinflammatory macrophage function in a model of *Helicobacter pylori* inflammation.[42] Similarly, conditional knockout of *Odc1* suggested a role of the enzyme in the polarization of T cells toward specified functional subsets.[17]

The aforementioned studies indicate a role of ODC in immune cell types and might provide an explanation for the reduced incidence of autoimmune diabetes seen in mice administered the ODC inhibitor DFMO.[11] Nevertheless, our prior studies[11,12,19,34] suggest a possible β cell-autonomous mechanism of action for polyamines, particularly through their downstream effects on eIF5A hypusination, in β cell proteome maintenance during diabetes development. In this study, the β cell-specific deletion of *Odc1* in mice resulted in no glycemic phenotype in young, healthy mice, but these results do not preclude a role (positive or negative) under conditions of stress. Therefore, we observed that *Odc1*$\Delta\beta$ mice exhibit relative preservation of β cell mass and delay in diabetes development in animals receiving multiple low-dose STZ, a DNA alkylating agent known to generate islet inflammation.[12,31,32] Our studies of ODC inhibition with DFMO in humans provide further clinical proof of principle of β cell autonomous effects of ODC in the setting of inflammation and demonstrate the largely proteome-driven response (as opposed to transcriptome response). Most notably, the proteomic response clusters along pathways beginning at mRNA translation to the transport and posttranslational modification of proteins in the endoplasmic reticulum and Golgi complex and ending with the formation and docking of secretory vesicles. These pathways are crucial for the synthesis and release of insulin and have also been implicated in antigen and major histocompatibility complex (MHC) class I production during the initiation or propagation of β-cell autoimmunity.[38,43]

To test the safety, tolerability, and potential efficacy of DFMO in T1D, we conducted a multicenter, randomized, placebo-controlled trial in pediatric (age 12 and over) and adult individuals with recent-onset T1D (diagnosed within the past 240 days). Our study showed that oral administration of DFMO to inhibit polyamine biosynthesis over a 3-month period is safe and well tolerated. Urinary polyamine data showed that active drug treatment engaged its target to inhibit ODC activity effectively, as reflected by dose-dependent reductions in urinary putrescine levels. Furthermore, although not powered to detect metabolic efficacy, participants on higher DFMO dose regimens (750 mg/m^2 and 1,000 mg/m^2/day) exhibited higher C-peptide AUC 6 months after treatment compared with placebo-treated participants. These findings suggest that, at the higher dosing regimens tested, DFMO may provide metabolic benefits to preserve β cell function and health in T1D.

A benefit of DMFO as a repurposed potential therapeutic in T1D is that safety and side effect profiles of multiple dose

Table 4. Efficacy measures

Measure	3-month time point			6-month time point		
	Drug dose (mg/m^2)	Least square means (95% CI)	p Value	Drug dose (mg/m^2)	Least square means (95% CI)	p Value
C-peptide AUC (ng/mL)	0	77,779.4 (63,857.3, 91,701.5)	–	0	68,459.5 (53742.1, 83,176.9)	–
	125	86,367.7 (69,073.5, 103,662)	0.43	125	97,850.1 (78,138.8, 117,561)	0.02
	250	86,172.6 (69,109.2, 103,236)	0.44	250	74,006.9 (55,971.6, 92,042.2)	0.63
	500	64,785.5 (47,546.9, 82,024.0)	0.24	500	66,049.5 (47,911.3, 84,187.6)	0.84
	750	94,202.8 (76,970.0, 111,436)	0.14	750	95,403.0 (77,270.5, 113,535)	0.03
	1,000	85,819.7 (68,802.7, 102,837)	0.46	1,000	95,669.7 (77,723.8, 113,616)	0.02
Glucose AUC (mg/dL)	0	29,942.2 (25,244.9, 34,639.5)	–	0	33,248.8 (29,487.0, 37,010.6)	–
	125	26,897.6 (21,497.9, 32,297.3)	0.39	125	26,620.4 (21,881.8, 31,359.0)	0.03
	250	35,420.3 (30,027.0, 40,813.7)	0.13	250	34,989.6 (30,670.3, 39,309.0)	0.54
	500	30,169.9 (24,667.5, 35,672.2)	0.95	500	31,412.8 (27,006.0, 35,819.6)	0.54
	750	28,057.8 (22,456.2, 33,659.5)	0.62	750	25,814.6 (21,328.1, 30,301.0)	0.02
	1,000	29,841.5 (24,447.8, 35,235.1)	0.98	1,000	30,633.3 (26,313.8, 34,952.9)	0.36
Fasting PI:C ratio (%)	0	1.2 (−2.3, 4.7)	–	0	1.3 (0.8, 1.8)	–
	125	6.1 (1.8, 10.3)	0.08	125	1.2 (0.6, 1.8)	0.69
	250	1.8 (−2.9, 6.5)	0.84	250	1.8 (1.1, 2.5)	0.30
	500	1.5 (−2.8, 5.7)	0.93	500	1.0 (0.4, 1.6)	0.43
	750	0.2 (−4.3, 4.7)	0.70	750	0.9 (0.2, 1.5)	0.26
	1,000	1.6 (−2.9, 6.1)	0.90	1000	0.4 (−0.2, 1.1)	0.04

Least square means adjusted for baseline value.
AUC, area under the curve; PI:C, proinsulin:C-peptide.

levels and regimens are available, including in children. Common anticipated risks of taking DFMO included gastrointestinal side effects, such as nausea, vomiting, abdominal pain, and diarrhea. Mild gastrointestinal symptoms were noted in some participants in our study. However, these episodes were typically self-limited and did not result in study withdrawal for any participants. Another previously noted but less likely side effect is myelosuppression; however, our findings suggest that white blood cell counts were similar between the placebo and active drug groups. Rash (diffuse urticaria) was noted in one participant. Other less likely possible side effects that were not reported in our cohort include hair loss, reversible hearing loss ($\leq$20%), and seizures (<2–3%). Side effects may have been less common in our cohort because prior reports have been primarily based on experience in children with cancer treated at higher doses (>3 g/m^2/day) who had other comorbidities and concomitant medication use and aberrant baseline blood counts.[44]

Although higher dosing regimens of DFMO were associated with higher C-peptide AUC compared with placebo at the end-of-study follow-up, we only noted significant changes in the PI:C (a marker of β cell stress) in the 1,000 mg/m^2 dosing group. This finding could reflect baseline differences in β cell stress, which can greatly vary, even at the time of T1D diagnosis.[36] Indeed, analysis of the entire study population showed that the 750 mg/m^2 dosing group had baseline PI:C values that fell below the median PI:C. In contrast, 6 of 6 individuals in the 1,000 mg/m^2 group had baseline values that were above the median of the entire population, suggesting a high baseline level of β cell stress. Nevertheless, the higher PI:C ratio in the highest-dose group is consistent with the finding from our proteomics analysis of cytokine-treated human islets that pathways related to protein processing and translocation appear altered upon DFMO treatment. In future studies, sample sizes that are large enough to ensure randomization of individuals with high and low baseline PI:C to active drug and placebo groups will be important to test whether baseline PI:C values are associated with ultimate treatment response.

In this study, DFMO treatment was not associated with changes in peripheral blood immune cell profiles at the end of treatment. Given the systemic administration of DFMO, this outcome may seem unexpected based on preclinical data showing effects of ODC inhibition or knockout on innate and adaptive immune cell subsets[17,42] and in NOD mice in which Treg cell subsets were increased and Th17 cell subsets were reduced in the pancreatic lymph node upon DFMO treatment.[11] Examination of immune cell effects at multiple time points in larger studies and follow up functional testing of immune cells will be important to confirm this finding. Taken together, this study suggests that DFMO is a safe oral treatment option that may improve β cell function and/or survival and may be a good choice in combination with immunomodulatory agents to augment β cell function and survival in T1D. A key next step will be implementation of an ongoing larger clinical study (ClinicalTrials.gov: NCT05594563) fully powered to detect a DFMO treatment effect on maintenance of C-peptide either in the recent-onset or at-risk population. Based on these results, DFMO could potentially also be applied to T1D prevention, likely as a combination therapy.

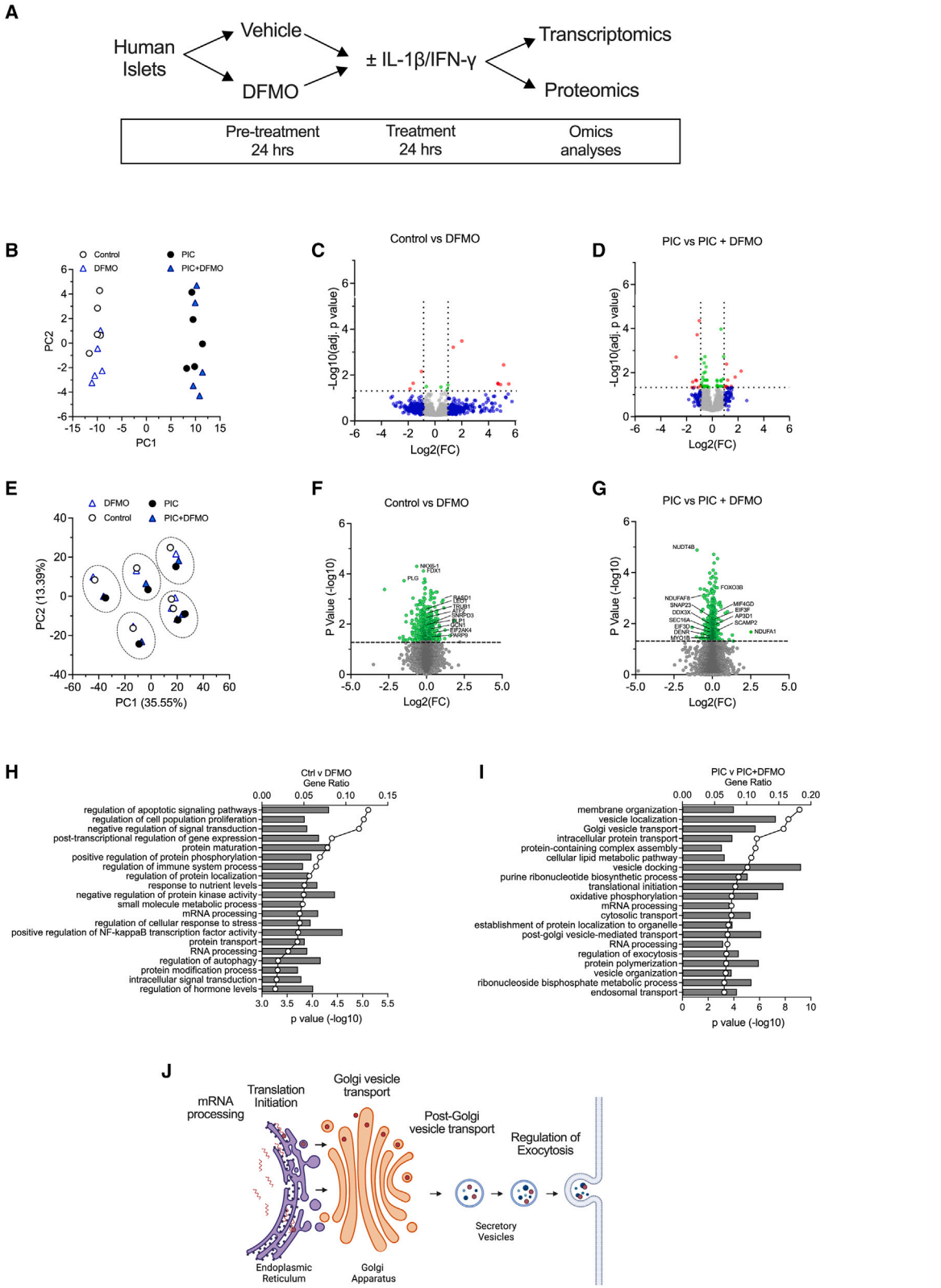

(legend on next page)

Limitations of study

Some limitations to our study should be acknowledged. First, although our animal studies were specifically designed to examine a β cell-autonomous effect of ODC in a model of islet inflammation, they were performed in the context of a mouse background that does not develop autoimmune diabetes. Therefore, it remains unclear whether β cell effects of the knockout would be observed in the setting of autoimmunity. The clinical study was designed to assess safety across a range of DFMO doses; thus, sample sizes for each dosing group were small, and all efficacy analyses were exploratory. Significant between-group differences in C-peptide AUC were not observed at the 3-month time point, only 6 months after randomization, after the placebo group had undergone further metabolic deterioration. However, observations showing the largest effect with the highest DFMO doses, where urinary putrescine levels were the most reduced, are reassuring for a true dose-response relationship. Furthermore, the finding that a benefit was detected after stopping the drug could be suggestive of a durable effect of DFMO treatment (an effect that was observed in a previous mouse study of DFMO administration).[11]

STAR★METHODS

Detailed methods are provided in the online version of this paper and include the following:

- KEY RESOURCES TABLE
- RESOURCE AVAILABILITY
  - Lead contact
  - Materials availability
  - Data and code availability
- EXPERIMENTAL MODEL AND STUDY PARTICIPANT DETAILS
  - Mice
  - Human islets
  - Human subjects
- METHOD DETAILS
  - Animal studies and pancreas immunohistochemistry
  - Human islet incubations, RNA sequencing, and proteomics
  - Clinical trial study design
  - Safety and monitoring
  - Clinical assays
- QUANTIFICATION AND STATISTICAL ANALYSIS
- ADDITIONAL RESOURCES

SUPPLEMENTAL INFORMATION

Supplemental information can be found online at https://doi.org/10.1016/j.xcrm.2023.101261.

ACKNOWLEDGMENTS

This study was supported by the JDRF (3-SRA-2015-7-M-R) (to L.A.D.), a Diabetes Research Connection award (to A.K.), and NIH grants UL1 TR002529 (to Indiana University), R01 DK121929 and R01DK133881 (to E.K.S.), R01 DK121987 and JDRF 5-CDA-2016-194-A-N (to T.L.M.), R01 DK060581 and R01 DK124906 (to R.G.M.), U01 DK127786 (to R.G.M. and C.E.-M.), and T32 AI153020 (to J.R.E.). This study used core services provided by Indiana Diabetes Research Center grant P30 DK097512 (to Indiana University School of Medicine) and Diabetes Research and Training Center grant P30 DK020595 (to the University of Chicago). Drug/placebo were supplied by Cancer Prevention Pharmaceuticals. These data were presented in part at Immunology of Diabetes Society (IDS), Network for Pancreatic Organ Donors with Diabetes (nPOD) and Pediatric Endocrine Society (PES) meetings. This work was also supported by grant 2021258 from the Doris Duke Charitable Foundation through the COVID-19 Fund to Retain Clinical Scientists collaborative grant program and was made possible through the support of grant 62288 from the John Templeton Foundation. We acknowledge Sheila Scheiding of the Benaroya Research Institute Human Immunophenotyping Core for data collection; Thien-Son Nguyen of the Benaroya Research Institute Clinical Core for sample processing; Alice Wiedeman of the Benaroya Research Institute for assistance with figures; Dr. Charanya Muralidharan and Jennifer Nelson at the University of Chicago for assistance with analysis of the immunostaining; Marina A. Gritsenko from the Pacific Northwest National Laboratory Biological Science Division for assistance with sample preparation for proteomic analysis; and Joanna Kramer from Medical College of Wisconsin and Amanda House and Emily Tabacxynski from University at Buffalo for serving as lead coordinators. The opinions expressed in this publication are those of the author(s) and do not necessarily reflect the view of the funding agencies. BioRender was used to create images in several of the figures and the graphical abstract.

AUTHOR CONTRIBUTIONS

E.K.S., L.A.D., and R.G.M. helped implement the clinical study, planned analyses, interpreted data, and wrote the manuscript. A.K., B.H., T.L.M., E.S.N., S.S., and S.A.T. planned analyses, performed experiments, and interpreted data. A.H. planned analyses and interpreted data. S.E.W., S.C., and L.D.M. helped implement the clinical study. S.M.P. helped implement the clinical study and planned and performed analyses. F.O., J.R.E., and B.-J.W.-R. performed analyses. C.E.-M. helped implement the clinical study. S.A.L., L.B., B.-J.W.-R., and J.R.E. performed and interpreted analyses. E.W.G. helped implement the study, and interpreted analyses. All authors edited the manuscript and approved the final version of the manuscript.

Figure 3. RNA sequencing and liquid chromatography-tandem mass spectrometry (LC-MS/MS) proteomics of human islets treated with DFMO and/or proinflammatory cytokines

(A) Human islets isolated from 5–6 cadaveric donors were pretreated with either vehicle or 5 mM DFMO, then incubated with or without proinflammatory cytokines (PICs; IL-1β and IFN-γ) for 24 h, followed by either unbiased RNA sequencing or proteomics.
(B) Principal-component analysis plot of RNA sequencing data.
(C) Volcano plot of differentially expressed genes in control vs. DFMO-treated islets.
(D) Volcano plot of differentially expressed genes in PIC vs. PIC plus DFMO-treated islets.
(E) Principal-component analysis plot of proteomics data. Circles identify clustering of individual donors.
(F) Volcano plot of differentially expressed proteins in control vs. DFMO-treated islets.
(G) Volcano plot of differentially expressed proteins in PIC vs. PIC plus DFMO-treated islets.
(H) GO biological process pathway analysis of differently expressed proteins of control vs. DFMO-treated islets.
(I) GO biological process pathway analysis of differently expressed proteins of PIC vs. PIC plus DFMO-treated islets.
(J) Commonly altered genes between transcriptomics and proteomics in PIC vs. PIC plus DFMO-treated islets. n = 5–6 biological replicates.

DECLARATION OF INTERESTS

R.G.M., L.A.D., and E.W.G. are coauthors on a patent application using DFMO for treatment of β cell dysfunction in T1D. E.W.G. is an employee of Cancer Prevention Pharmaceuticals.

Received: March 23, 2023
Revised: July 18, 2023
Accepted: October 5, 2023
Published: November 1, 2023

REFERENCES

1. DiMeglio, L.A., Evans-Molina, C., and Oram, R.A. (2018). Type 1 diabetes. Lancet *391*, 2449–2462. https://doi.org/10.1016/S0140-6736(18)31320-5.
2. Sims, E.K., Carr, A.L.J., Oram, R.A., DiMeglio, L.A., and Evans-Molina, C. (2021). 100 years of insulin: celebrating the past, present and future of diabetes therapy. Nat. Med. *27*, 1154–1164. https://doi.org/10.1038/s41591-021-01418-2.
3. Foster, N.C., Beck, R.W., Miller, K.M., Clements, M.A., Rickels, M.R., DiMeglio, L.A., Maahs, D.M., Tamborlane, W.V., Bergenstal, R., Smith, E., et al. (2019). State of Type 1 Diabetes Management and Outcomes from the T1D Exchange in 2016-2018. Diabetes Technol. Therapeut. *21*, 66–72. https://doi.org/10.1089/dia.2018.0384.
4. Rawshani, A., Sattar, N., Franzén, S., Rawshani, A., Hattersley, A.T., Svensson, A.M., Eliasson, B., and Gudbjörnsdottir, S. (2018). Excess mortality and cardiovascular disease in young adults with type 1 diabetes in relation to age at onset: a nationwide, register-based cohort study. Lancet *392*, 477–486. https://doi.org/10.1016/S0140-6736(18)31506-X.
5. Livingstone, S.J., Levin, D., Looker, H.C., Lindsay, R.S., Wild, S.H., Joss, N., Leese, G., Leslie, P., McCrimmon, R.J., Metcalfe, W., et al. (2015). Estimated life expectancy in a Scottish cohort with type 1 diabetes, 2008-2010. JAMA *313*, 37–44. https://doi.org/10.1001/jama.2014.16425.
6. Tao, B., Pietropaolo, M., Atkinson, M., Schatz, D., and Taylor, D. (2010). Estimating the cost of type 1 diabetes in the U.S.: a propensity score matching method. PLoS One *5*, e11501. https://doi.org/10.1371/journal.pone.0011501.
7. Jeyam, A., Colhoun, H., McGurnaghan, S., Blackbourn, L., McDonald, T.J., Palmer, C.N.A., McKnight, J.A., Strachan, M.W.J., Patrick, A.W., Chalmers, J., et al. (2021). Clinical Impact of Residual C-Peptide Secretion in Type 1 Diabetes on Glycemia and Microvascular Complications. Diabetes Care *44*, 390–398. https://doi.org/10.2337/dc20-0567.
8. Greenbaum, C., VanBuecken, D., and Lord, S. (2019). Disease-Modifying Therapies in Type 1 Diabetes: A Look into the Future of Diabetes Practice. Drugs *79*, 43–61. https://doi.org/10.1007/s40265-018-1035-y.
9. Sims, E.K., Mirmira, R.G., and Evans-Molina, C. (2020). The role of beta-cell dysfunction in early type 1 diabetes. Curr. Opin. Endocrinol. Diabetes Obes. *27*, 215–224. https://doi.org/10.1097/MED.0000000000000548.
10. Brooks, W.H. (2012). Autoimmune diseases and polyamines. Clin. Rev. Allergy Immunol. *42*, 58–70. https://doi.org/10.1007/s12016-011-8290-y.
11. Tersey, S.A., Colvin, S.C., Maier, B., and Mirmira, R.G. (2014). Protective effects of polyamine depletion in mouse models of type 1 diabetes: implications for therapy. Amino Acids *46*, 633–642. https://doi.org/10.1007/s00726-013-1560-7.
12. Maier, B., Ogihara, T., Trace, A.P., Tersey, S.A., Robbins, R.D., Chakrabarti, S.K., Nunemaker, C.S., Stull, N.D., Taylor, C.A., Thompson, J.E., et al. (2010). The unique hypusine modification of eIF5A promotes islet beta cell inflammation and dysfunction in mice. J. Clin. Invest. *120*, 2156–2170. https://doi.org/10.1172/JCI38924.
13. Kulkarni, A., Anderson, C.M., Mirmira, R.G., and Tersey, S.A. (2022). Role of Polyamines and Hypusine in β-cells and Diabetes Pathogenesis. Metabolites *12*, 344. https://doi.org/10.3390/metabo12040344.
14. Hesterberg, R.S., Cleveland, J.L., and Epling-Burnette, P.K. (2018). Role of Polyamines in Immune Cell Functions. Med. Sci. *6*, 22. https://doi.org/10.3390/medsci6010022.
15. Colvin, S.C., Maier, B., Morris, D.L., Tersey, S.A., and Mirmira, R.G. (2013). Deoxyhypusine synthase promotes differentiation and proliferation of T helper type 1 (Th1) cells in autoimmune diabetes. J. Biol. Chem. *288*, 36226–36235. https://doi.org/10.1074/jbc.M113.473942.
16. Tan, T.C.J., Kelly, V., Zou, X., Wright, D., Ly, T., and Zamoyska, R. (2022). Translation factor eIF5a is essential for IFNγ production and cell cycle regulation in primary CD8(+) T lymphocytes. Nat. Commun. *13*, 7796. https://doi.org/10.1038/s41467-022-35252-y.
17. Puleston, D.J., Baixauli, F., Sanin, D.E., Edwards-Hicks, J., Villa, M., Kabat, A.M., Kamiński, M.M., Stanckzak, M., Weiss, H.J., Grzes, K.M., et al. (2021). Polyamine metabolism is a central determinant of helper T cell lineage fidelity. Cell *184*, 4186–4202.e20. https://doi.org/10.1016/j.cell.2021.06.007.
18. Karacay, C., Prietl, B., Harer, C., Ehall, B., Haudum, C.W., Bounab, K., Franz, J., Eisenberg, T., Madeo, F., Kolb, D., et al. (2022). The effect of spermidine on autoimmunity and beta cell function in NOD mice. Sci. Rep. *12*, 4502. https://doi.org/10.1038/s41598-022-08168-2.
19. Robertson, M.A., Padgett, L.R., Fine, J.A., Chopra, G., and Mastracci, T.L. (2020). Targeting polyamine biosynthesis to stimulate beta cell regeneration in zebrafish. Islets *12*, 99–107. https://doi.org/10.1080/19382014.2020.1791530.
20. Pegg, A.E. (2016). Functions of Polyamines in Mammals. J. Biol. Chem. *291*, 14904–14912. https://doi.org/10.1074/jbc.R116.731661.
21. Priotto, G., Pinoges, L., Fursa, I.B., Burke, B., Nicolay, N., Grillet, G., Hewison, C., and Balasegaram, M. (2008). Safety and effectiveness of first line eflornithine for Trypanosoma brucei gambiense sleeping sickness in Sudan: cohort study. BMJ *336*, 705–708. https://doi.org/10.1136/bmj.39485.592674.BE.
22. Wolf, J.E., Jr., Shander, D., Huber, F., Jackson, J., Lin, C.S., Mathes, B.M., and Schrode, K.; Eflornithine HCl Study Group (2007). Randomized, double-blind clinical evaluation of the efficacy and safety of topical eflornithine HCl 13.9% cream in the treatment of women with facial hair. Int. J. Dermatol. *46*, 94–98. https://doi.org/10.1111/j.1365-4632.2006.03079.x.
23. LoGiudice, N., Le, L., Abuan, I., Leizorek, Y., and Roberts, S.C. (2018). Alpha-Difluoromethylornithine, an Irreversible Inhibitor of Polyamine Biosynthesis, as a Therapeutic Strategy against Hyperproliferative and Infectious Diseases. Med. Sci. *6*, 12. https://doi.org/10.3390/medsci6010012.
24. Laukaitis, C.M., and Gerner, E.W. (2011). DFMO: targeted risk reduction therapy for colorectal neoplasia. Best Pract. Res. Clin. Gastroenterol. *25*, 495–506. https://doi.org/10.1016/j.bpg.2011.09.007.
25. Saulnier Sholler, G.L., Gerner, E.W., Bergendahl, G., MacArthur, R.B., VanderWerff, A., Ashikaga, T., Bond, J.P., Ferguson, W., Roberts, W., Wada, R.K., et al. (2015). A Phase I Trial of DFMO Targeting Polyamine Addiction in Patients with Relapsed/Refractory Neuroblastoma. PLoS One *10*, e0127246. https://doi.org/10.1371/journal.pone.0127246.
26. Sholler, G.L.S., Ferguson, W., Bergendahl, G., Bond, J.P., Neville, K., Eslin, D., Brown, V., Roberts, W., Wada, R.K., Oesterheld, J., et al. (2018). Maintenance DFMO Increases Survival in High Risk Neuroblastoma. Sci. Rep. *8*, 14445. https://doi.org/10.1038/s41598-018-32659-w.
27. Kreul, S.M., Havighurst, T., Kim, K., Mendonça, E.A., Wood, G.S., Snow, S., Borich, A., Verma, A., and Bailey, H.H. (2012). A phase III skin cancer chemoprevention study of DFMO: long-term follow-up of skin cancer events and toxicity. Cancer Prev. Res. *5*, 1368–1374. https://doi.org/10.1158/1940-6207.CAPR-12-0233.
28. Burke, C.A., Dekker, E., Lynch, P., Samadder, N.J., Balaguer, F., Hüneburg, R., Burn, J., Castells, A., Gallinger, S., Lim, R., et al. (2020). Eflornithine plus Sulindac for Prevention of Progression in Familial Adenomatous Polyposis. N. Engl. J. Med. *383*, 1028–1039. https://doi.org/10.1056/NEJMoa1916063.

29. Levin, V.A., Ictech, S.E., and Hess, K.R. (2018). Clinical importance of eflornithine (alpha-difluoromethylornithine) for the treatment of malignant gliomas. CNS Oncol. *7*, CNS16. https://doi.org/10.2217/cns-2017-0031.

30. Tamarina, N.A., Roe, M.W., and Philipson, L. (2014). Characterization of mice expressing Ins1 gene promoter driven CreERT recombinase for conditional gene deletion in pancreatic β-cells. Islets *6*, e27685. https://doi.org/10.4161/isl.27685.

31. Calderon, B., Suri, A., Miller, M.J., and Unanue, E.R. (2008). Dendritic cells in islets of Langerhans constitutively present beta cell-derived peptides bound to their class II MHC molecules. Proc. Natl. Acad. Sci. USA *105*, 6121–6126. https://doi.org/10.1073/pnas.0801973105.

32. Lukić, M.L., Stosić-Grujicić, S., and Shahin, A. (1998). Effector mechanisms in low-dose streptozotocin-induced diabetes. Dev. Immunol. *6*, 119–128. https://doi.org/10.1155/1998/92198.

33. Tersey, S.A., Nishiki, Y., Templin, A.T., Cabrera, S.M., Stull, N.D., Colvin, S.C., Evans-Molina, C., Rickus, J.L., Maier, B., and Mirmira, R.G. (2012). Islet beta-cell endoplasmic reticulum stress precedes the onset of type 1 diabetes in the nonobese diabetic mouse model. Diabetes *61*, 818–827. https://doi.org/10.2337/db11-1293.

34. Levasseur, E.M., Yamada, K., Piñeros, A.R., Wu, W., Syed, F., Orr, K.S., Anderson-Baucum, E., Mastracci, T.L., Maier, B., Mosley, A.L., et al. (2019). Hypusine biosynthesis in β-cells links polyamine metabolism to facultative cellular proliferation to maintain glucose homeostasis. Sci. Signal. *12*, eaax0715. https://doi.org/10.1126/scisignal.aax0715.

35. Sims, E.K., Chaudhry, Z., Watkins, R., Syed, F., Blum, J., Ouyang, F., Perkins, S.M., Mirmira, R.G., Sosenko, J., DiMeglio, L.A., and Evans-Molina, C. (2016). Elevations in the Fasting Serum Proinsulin-to-C-Peptide Ratio Precede the Onset of Type 1 Diabetes. Diabetes Care *39*, 1519–1526. https://doi.org/10.2337/dc15-2849.

36. Watkins, R.A., Evans-Molina, C., Terrell, J.K., Day, K.H., Guindon, L., Restrepo, I.A., Mirmira, R.G., Blum, J.S., and DiMeglio, L.A. (2016). Proinsulin and heat shock protein 90 as biomarkers of beta-cell stress in the early period after onset of type 1 diabetes. Transl. Res. *168*, 96–106.e1. https://doi.org/10.1016/j.trsl.2015.08.010.

37. Dever, T.E., and Ivanov, I.P. (2018). Roles of polyamines in translation. J. Biol. Chem. *293*, 18719–18729. https://doi.org/10.1074/jbc.TM118.003338.

38. Kulkarni, A., Muralidharan, C., May, S.C., Tersey, S.A., and Mirmira, R.G. (2022). Inside the β-cell: Molecular Stress Response Pathways in Diabetes Pathogenesis. Endocrinology *164*, bqac184. https://doi.org/10.1210/endocr/bqac184.

39. Hougaard, D.M., and Larsson, L.I. (1986). Localization and possible function of polyamines in protein and peptide secreting cells. Med. Biol. *64*, 89–94.

40. Hougaard, D.M., Nielsen, J.H., and Larsson, L.I. (1986). Localization and biosynthesis of polyamines in insulin-producing cells. Biochem. J. *238*, 43–47. https://doi.org/10.1042/bj2380043.

41. Pendeville, H., Carpino, N., Marine, J.C., Takahashi, Y., Muller, M., Martial, J.A., and Cleveland, J.L. (2001). The ornithine decarboxylase gene is essential for cell survival during early murine development. Mol. Cell Biol. *21*, 6549–6558. https://doi.org/10.1128/mcb.21.19.6549-6558.2001.

42. Hardbower, D.M., Asim, M., Luis, P.B., Singh, K., Barry, D.P., Yang, C., Steeves, M.A., Cleveland, J.L., Schneider, C., Piazuelo, M.B., et al. (2017). Ornithine decarboxylase regulates M1 macrophage activation and mucosal inflammation via histone modifications. Proc. Natl. Acad. Sci. USA *114*, E751-e760. https://doi.org/10.1073/pnas.1614958114.

43. Roep, B.O., Thomaidou, S., van Tienhoven, R., and Zaldumbide, A. (2021). Type 1 diabetes mellitus as a disease of the β-cell (do not blame the immune system?). Nat. Rev. Endocrinol. *17*, 150–161. https://doi.org/10.1038/s41574-020-00443-4.

44. Smith, K.J., and Skelton, H. (2006). alpha-Difluoromethylornithine, a polyamine inhibitor: its potential role in controlling hair growth and in cancer treatment and chemo-prevention. Int. J. Dermatol. *45*, 337–344. https://doi.org/10.1111/j.1365-4632.2006.01231.x.

45. Zhang, Y., Parmigiani, G., and Johnson, W.E. (2020). ComBat-seq: batch effect adjustment for RNA-seq count data. NAR Genom. Bioinform. *2*, lqaa078. https://doi.org/10.1093/nargab/lqaa078.

46. Love, M.I., Huber, W., and Anders, S. (2014). Moderated estimation of fold change and dispersion for RNA-seq data with DESeq2. Genome Biol. *15*, 550. https://doi.org/10.1186/s13059-014-0550-8.

47. Wickham, H., and Wickham, H. (2016). Data Analysis (Springer).

48. Tersey, S.A., Levasseur, E.M., Syed, F., Farb, T.B., Orr, K.S., Nelson, J.B., Shaw, J.L., Bokvist, K., Mather, K.J., and Mirmira, R.G. (2018). Episodic β-cell death and dedifferentiation during diet-induced obesity and dysglycemia in male mice. Faseb. J. *32*, fj201800150RR. https://doi.org/10.1096/fj.201800150RR.

49. Kong, A.T., Leprevost, F.V., Avtonomov, D.M., Mellacheruvu, D., and Nesvizhskii, A.I. (2017). MSFragger: ultrafast and comprehensive peptide identification in mass spectrometry-based proteomics. Nat. Methods *14*, 513–520. https://doi.org/10.1038/nmeth.4256.

50. Teo, G.C., Polasky, D.A., Yu, F., and Nesvizhskii, A.I. (2021). Fast Deisotoping Algorithm and Its Implementation in the MSFragger Search Engine. J. Proteome Res. *20*, 498–505. https://doi.org/10.1021/acs.jproteome.0c00544.

51. Demichev, V., Messner, C.B., Vernardis, S.I., Lilley, K.S., and Ralser, M. (2020). DIA-NN: neural networks and interference correction enable deep proteome coverage in high throughput. Nat. Methods *17*, 41–44. https://doi.org/10.1038/s41592-019-0638-x.

52. Gitelman, S.E., Bundy, B.N., Ferrannini, E., Lim, N., Blanchfield, J.L., DiMeglio, L.A., Felner, E.I., Gaglia, J.L., Gottlieb, P.A., Long, S.A., et al. (2021). Imatinib therapy for patients with recent-onset type 1 diabetes: a multicentre, randomised, double-blind, placebo-controlled, phase 2 trial. Lancet Diabetes Endocrinol. *9*, 502–514. https://doi.org/10.1016/S2213-8587(21)00139-X.

53. Haller, M.J., Schatz, D.A., Skyler, J.S., Krischer, J.P., Bundy, B.N., Miller, J.L., Atkinson, M.A., Becker, D.J., Baidal, D., DiMeglio, L.A., et al. (2018). Low-Dose Anti-Thymocyte Globulin (ATG) Preserves beta-Cell Function and Improves HbA1c in New-Onset Type 1 Diabetes. Diabetes Care *41*, 1917–1925. https://doi.org/10.2337/dc18-0494.

54. Moran, A., Bundy, B., Becker, D.J., DiMeglio, L.A., Gitelman, S.E., Goland, R., Greenbaum, C.J., Herold, K.C., Marks, J.B., Raskin, P., et al. (2013). Interleukin-1 antagonism in type 1 diabetes of recent onset: two multicentre, randomised, double-blind, placebo-controlled trials. Lancet *381*, 1905–1915. https://doi.org/10.1016/S0140-6736(13)60023-9.

55. Thompson, P.A., Wertheim, B.C., Zell, J.A., Chen, W.P., McLaren, C.E., LaFleur, B.J., Meyskens, F.L., and Gerner, E.W. (2010). Levels of rectal mucosal polyamines and prostaglandin E2 predict ability of DFMO and sulindac to prevent colorectal adenoma. Gastroenterology *139*, 797–805.e1. https://doi.org/10.1053/j.gastro.2010.06.005.

56. Matzke, M.M., Waters, K.M., Metz, T.O., Jacobs, J.M., Sims, A.C., Baric, R.S., Pounds, J.G., and Webb-Robertson, B.J.M. (2011). Improved quality control processing of peptide-centric LC-MS proteomics data. Bioinformatics *27*, 2866–2872. https://doi.org/10.1093/bioinformatics/btr479.

57. Webb-Robertson, B.J.M., McCue, L.A., Waters, K.M., Matzke, M.M., Jacobs, J.M., Metz, T.O., Varnum, S.M., and Pounds, J.G. (2010). Combined statistical analyses of peptide intensities and peptide occurrences improves identification of significant peptides from MS-based proteomics data. J. Proteome Res. *9*, 5748–5756. https://doi.org/10.1021/pr1005247.

58. Allison, D.B., Paultre, F., Maggio, C., Mezzitis, N., and Pi-Sunyer, F.X. (1995). The use of areas under curves in diabetes research. Diabetes Care *18*, 245–250. https://doi.org/10.2337/diacare.18.2.245.

STAR★METHODS

KEY RESOURCES TABLE

REAGENT or RESOURCE	SOURCE	IDENTIFIER
Antibodies		
Anti-insulin	ProteinTech	Cat# 28728-1-AP: RRID:AB_2883281
Anti-insulin	Agilent Dako	Cat#IR002: RRID: AB_2800361
Anti-ODC	ProteinTech	Cat#28728-1-AP:RRID: AB_2881200
Alexa Fluor 568 donkey anti-rabbit antibody	Invitrogen	CAT# A10042: RRID:AB_2534017
Alexa Fluor 488 donkey anti-guinea-pig antibody	Invitrogen	CAT# A10042: RRID:AB_2534017
Anti-CD38 (APC)	BD Biosciences	Cat# 560980, RRID:AB_10584324
Anti-CD19 (BB515)	BD Biosciences	Cat# 564456, RRID:AB_2744309
Anti-CD14 (APC-ef780)	eBio/Thermo Fisher	Cat# 47-0149-42, RRID:AB_1834358
Anti-CD123 (PE-cf594)	BD Biosciences	Cat# 562391, RRID:AB_11153664
Anti-CD304 (PE)	BioLegends	Cat# 354504, RRID:AB_11219194
Anti-CD56 (BUV395)	BD Biosciences	Cat# 563554, RRID:AB_2687886
Anti-CD27 (BV605)	BioLegends	Cat# 302830, RRID:AB_2561450
Anti-CD141 (BV510)	BD Biosciences	Cat# 563298, RRID:AB_2728103
Anti-CD3 (AF700)	BioLegends	Cat# 300424, RRID:AB_493741
Anti-HLA-DR (BV785)	BioLegends	Cat# 307642, RRID:AB_2563461
Anti-IgD (BB700)	BD Biosciences	Cat# 566538, RRID:AB_2744486
Anti-CD16 (BV711)	BioLegends	Cat# 302044, RRID:AB_2563802
Anti-CD86 (PE-cy7)	BioLegends	Cat# 305422, RRID:AB_2074981
Anti-CD274 (BV421)	BD Biosciences	Cat# 563738, RRID:AB_2738396
Anti-CD1c (BV650)	BD Biosciences	Cat# 742751, RRID:AB_2741017
Anti-TIGIT (APC)	eBio/Thermo Fisher	Cat# 17-9500-42, RRID:AB_2573305
Anti-CCR7 (BV510)	BioLegends	Cat# 353232, RRID:AB_2563866
Anti-CD127 (BV711)	BioLegends	Cat# 351328, RRID:AB_2562908
Anti-CD56 (BUV395)	BD Biosciences	Cat# 563554, RRID:AB_2687886
Anti-CD3 (BV605)	BioLegends	Cat# 317322, RRID:AB_2561911
Anti-CD4 (BB515)	BD Biosciences	Cat# 564419, RRID:AB_2744419
Anti-CCR6 (PerCP-Cy5.5)	BioLegends	Cat# 353406, RRID:AB_10918437
Anti-CD45RO (BV786)	BD Biosciences	Cat# 564290, RRID:AB_2738733
Anti-KLRG1 (PE-Cy7)	BioLegends	Cat# 367720, RRID:AB_2728363
Anti-CD45RA (BUV737)	BD Biosciences	Cat# 612846, RRID:AB_2870168
Anti-CD8 (Ax700)	BioLegends	Cat# 344724, RRID:AB_2562790
Anti-CD57 (APC-Vio770)	Miltentyi Biotec	Cat# 130-111-813, RRID:AB_2658756
Anti-PD-1 (BV650)	BioLegends	Cat# 329950, RRID:AB_2566362
Anti-EOMES (PE)	eBio/Thermo Fisher	Cat# 12-4877-42, RRID:AB_2572615
Anti-Ki67 (BV421)	BioLegends	Cat# 350506, RRID:AB_2563860
Anti-FoxP3 (PE-CF594)	BD Biosciences	Cat# 562421, RRID:AB_11153143
Biological samples		
Human Islets R420	University of Alberta Islet Core	RRID:SAMN23408101
Human Islets R421	University of Alberta Islet Core	RRID:SAMN23491186
Human Islets	IIDP	RRID: SAMN23958505
Human Islets R425	University of Alberta Islet Core	RRID: SAMN24925207
Human Islets R427	University of Alberta Islet Core	RRID: SAMN25221445
Human Islets	IIDP	RRID: SAMN25519947

(*Continued on next page*)

Continued

REAGENT or RESOURCE	SOURCE	IDENTIFIER
Human Islets R430	University of Alberta Islet Core	RRID:SAMN2583750
Human Islets	IIDP	RRID: SAMN25860454
Human Islets R434	University of Alberta Islet Core	RRID:SAMN26419385
Human Islets	IIDP	RRID: SAMN26527277
Chemicals, peptides, and recombinant proteins		
Tamoxifen	Sigma	T5648
Streptozotocin	Sigma	S0130
Paraformaldehyde, 16%	Electron Microscopy Science	15710
Unmasking solution	Vector labs	H3300
Horse blocking buffer	Vector labs	S-2012-50
Immpress reagent kit peroxidase conjugated anti-rabbit Ig	Vector labs	MP-7402
Vector DAB peroxidase substrate kit	Vector labs	SK-4100
Hematoxilin	Sigma	GHS216
Permount	Fisher Scientific	12-545M
DAPI	Thermo Fisher Scientific	D1306
DFMO	Sigma	D193
Recombinant IL-1β	R&D Systems	201-LB-005
Recombinant IFN-γ	R&D Systems	285-IF-100
Complete protease inhibitor cocktail	Sigma	5892791001
Endoproteinase LysC	VWR	103258–578
Trypsin	Promega	V5111
Putrescine dihydrochloride	Sigma	Cat# P6505, Lot# BCBV1888
N1-N12-Diacetylspermine-*n*-hydrochloride	TRC	Cat# D367005, Lot# 1-TKN-163-2
N1-Acetylspermidine (hydrochloride)	TRC	Cat# A187845, Lot# 2-SRE-124-3
N8-Acetylspermidine dihydrochloride	TRC	Cat# A188000, Lot# 3-SNM-109-1
Decarboxylatesd-S-adenosylmethionine Sulfate salt	TRC	Cat# D222000, Lot# 4-PYL-169-1
Creatinine	Sigma	Cat# C4255, Lot# SLB4791
1,4-Butane-d8-diamine 2HCL	CDN	Cat# D-3980, Lot# C-193
1,12-diacetylspermine-d6 xPFPA	Metabolon	Lot# 211-037-3
N1-Acetylspermine-d3 xHCl	Metabolon	Lot# 211-032-3
N8-Acetylspermine-d3 xHCl	Metabolon	Lot# 211-030-8
Decarboxylated-S-adenosylmethionine-d3 xAcOH	TRC	Cat# D222002, Lot# 6-SUM-73-1
Creatinine-d3 (methyl-d3)	CDN	Cat# D-3689, Lot# BC-264
Critical commercial assays		
RNAeasy Mini Kit	Qiagen	N/A
Deposited data		
Proteomics dataset	MassIVE	MassIVE: MSV000091431
RNA sequencing dataset	GEO	GSE226888
Experimental models: Organisms/strains		
Odc1^{loxP}	Raghavendra G Mirmira	N/A
B6.Cg-Tg(Ins1-cre/ERT)1Lphi/J	Jackson Laboratory	RRID:IMSR_JAX:204709
Oligonucleotides		
5′- CTG AGG AGC CCA GAG AGG ACA TC -3′ (forward)	IDT	*Odc1^{loxP}* distal forward
5′- GAA GCA CCC ATA CAA GCA TAC AC -3′ (reverse)	IDT	*Odc1^{loxP}* distal reverse
5′- AAT GCT AGT ACT GCA TGA AAG TTC C -3′ (forward)	IDT	*Odc1^{loxP}* proximal forward
5′- AAG TAG CCA GTA CAG GAA GAA CTG -3′ (reverse)	IDT	*Odc1^{loxP}* proximal reverse
Software and algorithms		
Rosalind	Onramp.Bio Software	N/A

(*Continued on next page*)

Continued

REAGENT or RESOURCE	SOURCE	IDENTIFIER
ComBat-Seq	Zhang et al.[45]	N/A
DESeq2	Love et al.[46]	N/A
Ggplot2	Wickham et al.[47]	N/A
GraphPad Prism version 9.5	GraphPad	N/A

RESOURCE AVAILABILITY

Lead contact

Further information and requests for resources and reagents should be directed to and will be fulfilled by the Lead Contact, Dr. Raghavendra G. Mirmira (mirmira@uchicago.edu).

Materials availability

All unique/stable reagents generated in this study are available from the lead contact with a completed Materials Transfer Agreement.

Data and code availability

- RNA sequencing data have been uploaded to the public repository GEO and proteomics data have been uploaded to the public repository MassIVE. Accession numbers are listed in the key resources table. Both are publicly available at the time of publication. Microscopy data reported in this paper will be shared by the lead contact upon request.
- This paper does not report original code.
- Any additional information required to reanalyze the data reported in this paper is available from the lead contact upon request.

EXPERIMENTAL MODEL AND STUDY PARTICIPANT DETAILS

Mice

Mice were maintained under pathogen-free conditions according to protocols approved by the University of Chicago Institutional Animal Care and Use Committee. All mice were group housed under normal 12h:12h light:dark cycles and ad lib fed standard mouse chow. Mice containing the *Odc1* allele(s) flanked by *loxP* sequences were crossed to *MIP1-CreERT* mice[30] to generate breeding colonies on the C57BL/6J background. Control mice included the following genotypes: $Odc1^{loxP/loxP}$;$MIP1\text{-}CreERT^{neg}$ and $Odc1^{+/+}$;*MIP1-CreERT*. $Odc1^{\Delta\beta}$ had the following genotype: $Odc1^{loxP/loxP}$;*MIP1-CreERT*. Littermates were used in all experiments. Male mice were used in this study owing to their sensitivity to STZ-induced diabetes. Experiments were started at 8 weeks of age.

Human islets

Human islets from non-diabetic donors were obtained from the Integrated Islet Distribution Program (IIDP) or the University of Alberta Diabetes Institute Islet Core. Both the IIDP and the Alberta Islet Core require consent from family members of deceased donors prior to islet procurement and distribution to qualified islet research labs. The use of primary human islets from deidentified organ donors was approved by the Institutional Review Board of the University of Chicago and is not considered human subjects research. Islets from both males and females were used in this research and characteristics of the donors are provided in Table S4.

Human subjects

Persons with recent-onset T1D (within 240 days of diagnosis) were enrolled at 3 clinical diabetes centers within the United States: Indiana University in Indianapolis, IN, Medical College of Wisconsin in Milwaukee, WI, and the University at Buffalo in Buffalo, NY. Inclusion criteria included: age 12–40 years at the time of randomization with a clinical diagnosis of T1D within the past 2–8 months; random non-fasting C-peptide concentration of >0.2 pmol/mL at screening; positive titer for at least one islet autoantibody (to insulin, glutamic acid decarboxylase 65 (GAD65), islet antigen 2 (IA-2), or zinc transporter-8 (ZnT8)); and no prior history of immunomodulatory therapy. Because of reported risks for reversible sensorineural hearing loss, only individuals with normal hearing, defined as pure-tone audiometry (<20 dB [dB] baseline thresholds for frequencies 250, 500, 1000, and 2000 Hz) were included. Persons who had other chronic diseases, were unable to swallow pills, or had hematologic abnormalities at screening based on local clinical lab reference ranges (anemia, leukopenia, neutropenia, thrombocytopenia) were excluded.

This trial was performed in accordance with the Declaration of Helsinki under an FDA investigational new drug application number IND124781. The study was approved by the Institutional Review Boards at each of the participating sites. All participants or their legal guardians provided written informed consent. Safety was reviewed by an independent data and safety monitoring board (DSMB).

METHOD DETAILS

Animal studies and pancreas immunohistochemistry

The following primers were used for genotyping mice with *Odc1*^{loxP} alleles to identify: a) the remaining sequence from the neomycin resistance gene and the distal *loxP* site: 5′- CTG AGG AGC CCA GAG AGG ACA TC -3′ (forward) and 5′- GAA GCA CCC ATA CAA GCA TAC AC -3′ (reverse), and were expected to generate a 477 base pair (bp) band for the wild-type allele and 619 bp for the *loxP*-containing allele; b) the proximal *loxP* site: 5′- AAT GCT AGT ACT GCA TGA AAG TTC C -3′ (forward) and 5′- AAG TAG CCA GTA CAG GAA GAA CTG -3′ (reverse), and were expected to generate a 411 bp band for the wild-type allele and 460 bp for the *loxP* allele. Prior to all experiments, mice were administered three daily intraperitoneal injections of 2.5 mg of tamoxifen dissolved in peanut oil at 8 weeks of age (to cause recombination of the *loxP* alleles). Mice were then allowed to acclimate for 1 week before further experimentation. STZ was administered intraperitoneally at a dose of 55 mg/kg body weight daily for 5 consecutive days. Blood glucose was monitored twice weekly using a hand-held glucometer (AlphaTrak) and a glucose tolerance test using 1 mg/kg glucose was performed 4 days after the last STZ treatment. Diabetes incidence was determined as a blood glucose value greater than 250 mg/dL.

Pancreata from at least 5 different mice per group were fixed in 4% paraformaldehyde, paraffin embedded, and sectioned onto glass slides. For β-cell mass, pancreata were immunostained using rabbit anti-insulin (1:1000; 28728-1-AP, ProteinTech), Immpress reagent kit peroxidase conjugated anti-rabbit Ig (Vector), and DAB peroxidase substrate kit (Vector). β-cell mass was calculated by measuring insulin positive area and pancreas area using CV-X software on a Keyence fluorescent microscope system (Keyence) as described previously.[48] For ODC quantification pancreata were stained for immunofluorescence using the following antibodies: anti-ODC (1:300; 28728-1-AP, Proteintech) and anti-insulin antibody (IR002, Dako). Alexa Fluor antibodies were used as secondary antibodies (Invitrogen). All samples were stained with DAPI for nuclei identification (Thermo Fisher Scientific, D1306). Immunostainings were quantified by counting the number of double ODC+ insulin+ cell. Images were acquired using an A1 (Nikon) confocal.

Human islet incubations, RNA sequencing, and proteomics

Upon receipt, human islets were cultured in fresh human islet medium (Prodo labs) and allowed to recover for 24 h. Hand-picked islets were distributed into culture wells for 4 conditions: Vehicle, 5 mM DFMO, proinflammatory cytokines (50 IU IL-1β + 1000 IU IFN-γ, R&D Systems), and proinflammatory cytokines +5 mM DFMO. The islets were pre-treated with 5 mM DFMO for 24 h prior to addition of proinflammatory cytokines. Incubation proceeded for another 24 h. After the completion of the treatments, the islets were washed twice with PBS. The pellets were then stored at −80°C until RNA-sequencing or proteomics. For RNA sequencing, RNA extraction was performed from the cell pellet following the RNeasy Mini kit instructions (Qiagen). Samples were submitted for library generation and sequencing at the University of Chicago sequencing core using a NovaSeq 6000 (Illumina). Fastq files were then initially processed with Rosalind (Onramp.Bio Software) for gene alignment and generation of raw counts matrix. Owing to high variability between human samples, raw counts were inputted into ComBat-Seq[45] for batch correction utilizing default parameters. Using the batch corrected matrix, DESeq2[46] was then used with the standard workflow for differential expression analysis. Subsequent data visualization was performed with ggplot2 and Prism version 9.5 for Mac (GraphPad Software).

Quantitative proteomics analysis was performed using the data-independent acquisition approach. Islet pellets were dissolved in lysis buffer (8 M Urea; 50 mM Tris pH 8.0; 75 mM NaCl; complete protease inhibitor cocktail (Sigma 5892791001). Disulfide bonds were reduced by adding 250 mM dithiothreitol to a final concentration of 5 mM. Samples were alkylated by adding 500 mM iodoacetamide to a final concentration of 40 mM. Samples were diluted 4-fold with 50 mM Tris HCl (pH 8.0). Proteins were digested with an 1/50 (enzyme/protein) ratio of sequencing grade endoproteinase LysC (VWR) for 2 h at 37°C, followed by sequencing grade trypsin (Promega) overnight at 25°C. Reactions were quenched by adding 10% trifluoroacetic acid to a final concentration of 1%. Samples were desalted in C18 solid phase extraction plates (Phenomenex) and dried in a vacuum centrifuge. Peptide aliquots from each sample were pooled together to build a peptide library. For the peptide library, the pooled mixture was fractionated by high pH reverse phase chromatography, spiked with a retention time calibration peptide mix (iRT, Biognosys), and analyzed by liquid chromatography with tandem mass spectrometry (LC-MS/MS) on QExactive HF mass spectrometer (Thermo Fisher Scientific). Peptides were separated in a C18 column (70 cm × 75 μm i.d., Phenomenex Jupiter, 3 μm particle size, 300 Å pore size) connected to an Acquity M-Class Nano UHPLC system (Waters). Full MS spectra of eluting peptides were collected on a 300–1800 m/z range and the top 12 most intense parent ions were submitted to high-energy collision dissociation (isolation window 0.7 m/z, normalized collision energy 30) before being dynamically excluded for 30 s. Individual samples were analyzed by data-independent acquisition using the same separation gradient and mass spectrometer. Tandem mass spectra were collected from the range of 400–900 m/z with 10 m/z increment windows (10.0 m/z isolation width; 30% normalized collision energy; 70,000 resolution at 400 m/z). Post-LC-MS/MS, a hybrid peptide library was generated with MSFragger via Fragpipe.[49,50] The MS/MS spectra were searched against the human Swissprot database (July 31, 2021, 20,420 sequences) with an initial fragment mass tolerance of 20 ppm. Only fully tryptic peptides were considered with up to two missed cleavages. Carbamidomethylation of cysteine was set as a fixed modification; acetylation of protein N-terminus and oxidation of methionine residues were set as variable modifications. The final library contained peptides filtered with 1% false discovery rate (FDR) at protein, peptide, and peptide/spectrum match levels. The raw data was processed with DIA-NN[51] matching against the generated hybrid library, using an FDR of 1%.

Clinical trial study design

This dose-ranging study was a multicenter, double-blind, placebo-controlled, 2:1 random assigned, phase I/II clinic trial (Registered ClinicalTrials.gov number NCT02384889, no changes were made to approved trial design). Overall study design is summarized in Figure 2A, with a CONSORT diagram in Figure S2 and schedule of events in Table S1. Gender, race, ethnicity and age information are provided in Table 1. Data on ancestry and socioeconomic status were not collected. The prespecified primary study outcome was assessment of the safety of varying doses of DFMO. Prespecified secondary efficacy measurements were also obtained by analyzing β-cell function as assessed by endogenous C-peptide secretion area under the curve (AUC) in response to mixed meal tolerance tests (MMTTs) and changes in proinsulin to C-peptide ratios, a marker of β-cell stress.[35,52,53] Other prespecified outcomes included changes in mean glycemia, urine polyamines, stimulated C-peptide values, and changes in immune features.

After a <60 days run-in period, 41 individuals were randomized to 3-month treatment with either placebo or a fixed oral dose DFMO. For DFMO dosing, participants were randomly assigned to one of five sequential dose cohorts: 125 mg/m^2, 250 mg/m^2, 500 mg/m^2, 750 mg/m^2, or 1000 mg/m^2 per day. Participants randomized to DFMO treatment were first treated with the lowest dose, then after 6–7 participants had been randomized to that group (cohort enrollment halted each time the number randomized to DFMO reached n = 6), if no dose-limiting toxicity occurred, the next higher dosing regimen was utilized for subsequent participants randomized to DFMO treatment. Participants who failed to complete the 3 months of treatment with assessable data were replaced. Dose frequency was daily or twice daily depending on dosing regimen. All participants received bottles containing one hundred 250mg tablets of either placebo or active drug. Treatment assignments were double-masked at all doses except for the 6 subjects at the 1000 mg/m^2/day group, since no participants in that group were assigned to placebo.

Participants were randomly assigned in a 2:1 ratio, stratified by age (> or <18 years) to receive experimental treatment with DFMO or placebo. A computer-based randomization plan was prepared by the study statistician at Indiana University using a random number generator (PROC PLAN in SAS). Randomization lists were kept by the Indiana University Study Coordinating Center administrator and the study pharmacy (Eminent Services Corporation) and randomization was administered by the study pharmacy. Neither participants nor clinical research personnel were aware of the treatment assignments.

Safety and monitoring

The full schedule of events is in Table S1. All adverse events were recorded by study personnel and graded using the National Cancer Institute's Common Terminology Criteria for Adverse Events (CTCAE) version 4.0. Adverse events were reviewed by an internal data safety monitoring committee (DMC) at Indiana University after the last subject in each cohort completed 3 months of therapy, and before each successive cohort was enrolled. The Midwest Area Research Consortium for Health (MARCH) external independent data safety monitoring board (DSMB) also reviewed study safety data biannually (https://ctsi.mcw.edu/march/). Dose-limiting toxicities were defined *a priori* as any of the following events that were possibly, probably, or definitely attributable to DFMO therapy: Grade 3 thrombocytopenia (platelet count <50,000/mm^3), Grade 3 neutropenia (neutrophil count <1000/mm^3), Grade 3 anemia (hemoglobin $\leq$8.0 g/dL, or drop $\geq$2.0 g/dL and <10.0 g/dL), Grade 3 symptoms of nausea, abdominal pain, or diarrhea, or audiometric impairment, defined as $\geq$25dB hearing loss from baseline at 2 thresholds on audiogram. Rules for dose escalation to the next cohort were that less than 2 subjects in the prior cohort could report a dose-limiting toxicity judged to be related to treatment during the treatment or follow-up periods. Subjects who did not complete the 3-month treatment period for reasons other than toxicity were replaced by another subject in order of randomization schedule.

To assess for possible metabolic effects, 2-h mixed meal tolerance test (MMTT) was performed at the time of randomization, at the end of the 3-month treatment period, and after a 3-month wash-out period. For MMTTs, as previously described,[54] participants were given 6 mL/kg of Boost High Protein (Nestlé Nutrition, Vevey, Switzerland) to a maximum of 360 mL ingested within 5 min, and blood samples were taken at −10, 0, 15, 30, 60, 90, and 120 min after start of ingestion for analysis.

Clinical assays

Diagnostic islet autoantibody testing was performed by the Barbara Davis Center for Childhood Diabetes using radioimmunobinding assays (Aurora, Colorado). Hemoglobin A1c (HbA1c), complete blood counts (CBC) and comprehensive metabolic panels (CMP) were tested using respective hospital clinical laboratories. The Indiana University Diabetes Research Center Translation Core analyzed glucose using the glucose oxidase method (Randox Daytona clinical analyzer), C-peptide (TOSOH Bioscience), and intact proinsulin by ELISA (TECO Medical). High-performance liquid chromatography was performed as previously described to detect polyamines as their N-dansylated derivatives.[55]

Peripheral blood mononuclear cells (PBMCs) were collected, shipped and cryopreserved within 24 h of collection at baseline, 3- and 6-month timepoints. Samples were thawed and processed for immunophenotyping analysis at the Benaroya Research Institute (BRI) as previously described.[52] Briefly, previously validated panels and fluorochrome-conjugated antibodies were used with hierarchical gating to identify broad immune subsets, including CD4$^+$CD8$^+$ T cells and Tregs, CD19$^+$ B cells, monocytes/classical dendritic cells, and NK T cells, as well as memory subsets of B cells and T cells, and phenotyping markers for cell activation or regulation, including PDL1, CD86, HLA-DR, CD27, CD38, CCR6, TIGIT, KLRG1, PD1, EOMES, and Ki67. Immunophenotyping panels are described in Tables S7 and S8.

QUANTIFICATION AND STATISTICAL ANALYSIS

For human islet proteomics, data was log_2-transformed and subjected to quality control processing using a statistical outlier list developed for proteomics data that evaluates correlation and missing data, as well as sample level distributional properties of median absolute deviation, skew and kurtosis.[56] No outliers were identified, which was confirmed via visual inspection via Pearson correlation, boxplots, and Principal Components Analysis. Data were normalized to median total abundance. Statistics were performed using two tests to evaluate quantitative differences via a standard paired t-test and qualitative differences (presence/absence) via a g-test.[57] None of the protein groups failed a Kolmogorov-Smirnov test of normality based on the difference in abundance.

For the clinical study, sample sizes were based on the ability to detect dose-limiting toxicities. With 6 subjects per cohort in the DMFO group, the probably of observing at least 1 DLT within a cohort is greater than 0.80 if the true DLT rate is at least 25%. The Statistical Analysis plan included determination of DFMO dose effect of primary safety and secondary efficacy endpoints. Area under the curve values were calculated using the trapezoidal rule.[58] Fasting proinsulin:C-peptide (PI:C) ratios were calculated as equimolar ratios x 100. Given small sample sizes, prespecified efficacy analyses were considered exploratory. Endpoints of interest were analyzed for treatment effect using analysis of covariance (ANCOVA) models, with the change from baseline (or start of treatment) response modeled as a function of main effects for dose level, and the corresponding baseline response as a covariate. The 3- and 6-month time points were analyzed separately. The least squares means and associated 95% confidence intervals were used to describe the DMFO dose versus response relationships. Given that this was a pilot dose ranging study with relatively small samples sizes, impacts of individual participant features such as sex, gender, ancestry, race and ethnicity, socioeconomic status were not tested. p values < 0.05 were considered statistically significant.

ADDITIONAL RESOURCES

The trial described was pre-registered at Clinical Trials.gov (Registered ClinicalTrials.gov number NCT02384889): https://classic.clinicaltrials.gov/ct2/show/NCT02384889.